Published in final edited form as:
Nano Today. 2013 June 1; 8(3): 313–331. doi:10.1016/j.nantod.2013.04.006.

Anthracycline Nano-Delivery Systems to Overcome Multiple Drug Resistance: A Comprehensive Review

Ping Ma[1] and **Russell J. Mumper**[1,2,*]

[1]Center for Nanotechnology in Drug Delivery, Division of Molecular Pharmaceutics, UNC Eshelman School of Pharmacy, University of North Carolina at Chapel Hill, Chapel Hill, NC 27599, USA

[2]UNC Lineberger Comprehensive Cancer Center, University of North Carolina at Chapel Hill, NC 27599, USA

Abstract

Anthracyclines (doxorubicin, daunorubicin, and idarubicin) are very effective chemotherapeutic drugs to treat many cancers; however, the development of multiple drug resistance (MDR) is one of the major limitations for their clinical applications. Nano-delivery systems have emerged as the novel cancer therapeutics to overcome MDR. Up until now, many anthracycline nano-delivery systems have been developed and reported to effectively circumvent MDR both *in-vitro* and *in-vivo*, and some of these systems have even advanced to clinical trials, such as the HPMA-doxorubicin (HPMA-DOX) conjugate. Doxil, a DOX PEGylated liposome formulation, was developed and approved by FDA in 1995. Unfortunately, this formulation does not address the MDR problem. In this comprehensive review, more than ten types of developed anthracycline nano-delivery systems to overcome MDR and their proposed mechanisms are covered and discussed, including liposomes; polymeric micelles, conjugate and nanoparticles; peptide/protein conjugates; solid-lipid, magnetic, gold, silica, and cyclodextrin nanoparticles; and carbon nanotubes.

Keywords

anthracyclines; nanoparticles; multi-drug resistance

1. Anthracyclines in Cancer Treatment

Anthracyclines are among the most effective and commonly used chemotherapeutic drugs [1]. The mechanisms of antitumor activity of anthracyclines are well characterized and documented, wherein anthracyclines are able to diffuse across the cell membrane, intercalate between DNA base pairs, target topoisomerase II (TOPO II), and induce cell apoptosis [2]. The first anthracyclines of doxorubicin (DOX, Figure 1) and daunorubicin (DNR, Figure 1) were isolated from the bacterium of *Streptomyces peucetius*, which could produce a red

*Corresponding author: Russell J. Mumper, Ph.D., John A. McNeill Distinguished Professor, Center for Nanotechnology in Drug Delivery, Division of Molecular Pharmaceutics, UNC Eshelman School of Pharmacy, CB# 7355, 100G Beard Hall, University of North Carolina at Chapel Hill, Chapel Hill, North Carolina 27599-7355, mumper@email.unc.edu, Phone: (919) 966-1271, Fax: (919) 966-6919.

pigment and were found to have good activity against murine tumors back to the 1950s [3, 4]. DOX is widely used to treat various cancers, including leukemia, Hodgkin's lymphoma, bladder and breast cancers, etc., while DNR is used to treat some types of leukemias, such as acute myeloid leukemia (AML) and acute lymphocytic leukemia (ALL). In order to find better anthracyclines, a great deal of research has been conducted to establish the structure-activity relationship of anthracyclines, and this research has guided identification and synthesis of better anthracyclines. In last two decades there have been hundreds of DOX and DNR analogs reported in different laboratories wherein there have been chemical modifications of their tetracyclic ring, side chain, and/or aminosugar [5, 6]. However, only a few of the analogs have been approved for clinic use and among them, idarubicin (IDA, 4-demethoxydaunorubicin, Figure 1) is the most successful alternative to DNR [7]. Idarubicin was approved by the US FDA in 1990 [4]. The absence of the methoxy group at position 4 of IDA results in significantly enhanced lipophilicity, which results in more rapid cellular uptake, superior DNA-binding capacity, and consequently greater cytotoxicity as compared to DOX and DNR [2]. The physicochemical properties of these three anthracyclines are summarized in Table 1. For use in the clinic, they are formulated as hydrochloride salt forms dissolved in an aqueous solution for intravenous injection.

Unfortunately, the clinical use of anthracyclines has been limited by their severe cardiotoxicity and the development of multiple drug resistance (MDR) [8, 9]. In general, many patients achieve a complete remission when initially treated with anthracyclines; however, ~70% of the patients eventually experience a relapse of the disease, and the treatment failure is mainly due to MDR. The MDR mechanisms of anthracyclines are complicated and not fully understood. The most established mechanism of resistance is over-expression of drug efflux proteins, particularly members of the ATP-binding cassette (ABC) superfamily: P-glycoprotein (P-gp, MDR1), multidrug resistance protein 1 (MRP1), and breast cancer resistance protein (BCRP). Anthracyclines are known to be efficient substrates for ABC transporters. For example, P-gp, a membrane transporter encoded by MDR1 gene, actively pumps anthracyclines out of the cells resulting in drug resistance [10, 11]. Baekelandt et al. reported the correlation of P-gp expression and response rate in a study involving 73 patients with advanced ovarian cancer [12]. They found that P-gp negative patients responded significantly better to chemotherapy ($p < 0.001$), and the P-gp expression was clearly a predictor of both overall ($p = 0.045$) and progression free ($p = 0.006$) survival, which indicated P-gp expression was a marker for chemotherapy resistance and prognosis in advanced ovarian cancer. In addition to ABC transporters, other cellular mechanisms of resistance have also been reported, such as alteration in TOPO II, free-radical formation, up-regulation of B-cell lymphoma 2 (BCL-2) family members, down-regulation of tumor suppressor protein p53, etc. [13–16].

Non-cellular resistance mechanisms have also proposed and are attributed to the unique vasculatory of solid tumors [17–19]. The vasculature of solid tumors is characterized as heterogeneous, where the blood vessels are dilated and tortuous. The interstitial fluid pressure of solid tumors is increased than normal tissues, which is due to the higher vascular permeability and the absence of lymphatic system. In addition, solid tumors have an acidic environment and lack nutrients and oxygen, all of which help to induce resistance to cytotoxic drugs.

Nanoparticle (NP) delivery systems have been shown to be promising carriers to improve the therapeutic effect of anthracyclines mainly due to the enhanced permeability and retention (EPR) effect in solid tumors, while they minimize systemic exposure, enhance drug efficacy and reduce non-specific toxicity [20–22]. Nano-delivery systems have also been shown to increase the circulation time of drugs in blood, thereby increasing the ability of drugs to reach their sites of action. Doxil, a DOX-encapsulated polyethylene glycol

(PEG)-coated liposome formulation with the particle size of ~100 nm, was approved in 1995 for the treatment of ovarian cancer, AIDS-related Kaposi's sarcoma, and multiple myeloma. The DOX PEGylated liposomes demonstrate slower plasma clearance rate, prolonged circulation time in blood, and decreased volume of distribution than either traditional DOX liposomes or free DOX. Importantly, Doxil was proved to have less cardiotoxicity as compared to free DOX [23–25]. However, the liposome formulation has not addressed MDR which continues to be a major hurdle in cancer therapy. In order to overcome MDR, various nano-delivery systems have been developed and evaluated both *in-vitro* and *in-vivo*. In this comprehensive review, different nano-delivery systems for the delivery of anthracyclines as well as their mechanisms to overcome MDR are addressed (Table 2 and Figure 2).

2. Anthracycline Nanoparticles to Overcome MDR

2.1 Liposomes

Thierry and his colleagues developed DOX-encapsulated liposomes with cardiolipin/phosphatidylcholine/cholesterol (CL/PC/CHOL) and demonstrated that both DOX-encapsulated liposomes and free DOX spiked into a suspension of empty liposomes could reverse MDR and had comparable activity in MDR Chinese hamster LZ cells [26]. The efficacy of free DOX spiked into a suspension of empty liposomes was probably due to the high binding affinity ($1.6 \times 10^6\ M^{-1}$) of positively-charged DOX to the negatively-charged CL. However, neither pretreatment with empty liposomes before drug treatment nor the combination of vincristine and empty liposomes could reverse MDR, which suggested DOX must be incorporated or complexed with liposomes to overcome MDR. The authors suggested the DOX in liposomes would alter intracytoplasmic vesicles to transport DOX in MDR cells, and the modulation of MDR could be due to the increase of drug accumulation or the intracellular drug redistribution in MDR cells. Rahman et al. prepared DOX-loaded liposomes composed of CL/PC/CHOL (molar ratio 2:10:6.8) and compared the cytotoxicity of the liposomes versus free DOX in P-gp resistant HL-60/VCR and its parental HL-60 cell lines [27, 28]. The results showed that the IC_{50} values of free DOX (30 nM) and DOX liposomes (20 nM) were comparable in HL-60 cells, while in HL-60/VCR cells the IC_{50} values of free DOX and DOX liposomes were 0.9 and 0.17 μM, respectively, which indicated the liposome formulation was 5-fold more toxic than free DOX in HL-60/VCR cells. The mechanisms of DOX liposomes to overcome MDR were investigated, and it was concluded that the empty liposomes can directly interact with P-gp based on their competitive inhibition of [^{3}H]-vincristine binding to P-gp. In addition, the membrane fluidity of the resistant cells was different from that of the sensitive cells. Therefore, it was concluded that liposomes likely interact with and modify the environment of the plasma membrane, resulting in more drug uptake in resistant cells. In contrast, Hu et al. formulated three different DOX liposomes; however, none of them showed MDR circumvention *in-vitro* in rat glioblastoma cells, and the empty liposomes were unable to inhibit [^{3}H]-azidopine binding to P-gp [29]. It was suggested that the different results were due to the different compositions in the liposome formulations where they included lower amounts of lipids and higher DOX/lipid molar ratios. In addition, the origin of the lipids in liposomes was different. All of these may lead to avoidance of the interaction between lipids/liposomes and cell plasma membrane. More recently, Riganti et al. formulated DOX-containing anionic liposomes (Lipodox) and demonstrated that the Lipodox was significantly more effective than free DOX in resistant HT29-dx cells [30]. The P-gp inhibition mechanisms of Lipodox were summarized in two aspects: 1) indirect effect, which is due to the interaction between liposomes and cell membrane (e.g. change in the composition of lipid rafts and P-gp localization); 2) direct effect, which is due to the direct interaction between liposome and P-gp (e.g. direct inhibition of ATPase activity).

Co-delivery of DOX and a P-gp inhibitor was also reported to overcome MDR. Krishna et al. developed DOX liposomes with 1,2-distearoyl-sn-glycero-3-phosphocholine (DSPC) and CHOL at the lipid molar ratio of 55:45 [31]. The DOX liposomes or free DOX (i.v.) and P-gp inhibitor PSC 833 (p.o.) were co-administered in normal BDF1 mice. It was found that with p.o. administration of PSC 833, the maximum tolerated dose (MTD) was reduced by 2.5–3-fold with free drug while only 20% reduction for DOX liposomes compared to i.v. alone. This suggested the DOX liposomes were less toxic than free DOX. Furthermore, in a murine P388/ADR solid tumor model, the tumor inhibition of DOX liposomes combined with PSC 833 was comparable to the sensitive P388/WT tumors, while a modest modulation was observed for the co-administration of free DOX with PSC 833 at the MTD. It was also confirmed that the antitumor efficacy was PSC 833 dependent because the DOX liposomes alone provided significantly less activity. It should be noted that the DOX liposomes demonstrated a comparable pharmacokinetic profile and tissue biodistribution with or without PSC 833 p.o. administration, while free DOX altered pharmacokinetics in the presence of PSC 833. Similarly, Wang et al. co-encapsulated DOX and another P-gp inhibitor, verapamil, into stealth liposomes composed of egg phosphatidylcholine (EPC), CHOL, and PEG_{2000}-DSPE (molar ratio 50:45:5) [32]. The results showed the stealth liposomes with DOX and verapamil overcame MDR *in-vitro* in both DOX-resistant rat prostate cancer cell line Mat-LyLu-B2 and human uterus sarcoma MES-SA/DX5 cell line, while the stealth liposomes with DOX alone were not effective enough to reverse MDR. To further target the tumor cells, the Robert group synthesized transferrin immunoliposomes encapsulating both DOX and verapamil (Tf-L-DOX/VER), and this formulation increased the cytotoxicity by 5.2- and 2.8-fold over that of L-DOX/VER and Tf-L-DOX, respectively, in DOX-resistant K562 leukemia cells [33].

Since the mechanisms of MDR are multifactorial, the ideal delivery system should address different MDR pathways. In order to do so, the Minko group developed a complex liposome system which included: 1) a chemotherapeutic drug of DOX; 2) antisense oligonucleotides (ASOs) targeted to MDR1 mRNA; and 3) ASOs targeted to BCL-2 mRNA [34]. They showed this complex system was more toxic *in-vitro* in resistant A2870/AD human ovarian carcinoma cells when compared to free DOX, DOX liposomes, and DOX liposomes with either one type of ASOs. In addition, the complex liposomes were shown to be internalized into the cancer cells both *in-vitro* and *in-vivo* and even penetrated into the nucleus. However, the mechanisms were not clear. It was also suggested that both membrane fusion and endocytosis may be involved in liposome internalization into the tumor cells. Subsequently, the Minko group successfully prepared a series of complex liposomes for co-delivery of DOX and ASO targeted to hypoxia-inducible factor 1α (HIF1A) mRNA [35] or siRNA targeted to MRP1 and BCL-2 mRNA [36]. All of the liposome systems with the combination of DOX and ASO or siRNA showed enhanced chemotherapeutic efficacy in resistant cells both *in-vitro* and *in-vivo*. Chen et al. developed even more complex DOX liposome systems, namely cationic liposome-polycation-DNA (LPD) and anionic liposome-polycation-DNA (LPD-II), and showed a significant antitumor inhibition in an NCI/ADR-RES xenograft mouse model [37]. With their DOX liposome systems, they co-delivered the following cargos to overcome MDR: 1) a guanidinium-containing cationic lipid, N,N-distearyl-N-methyl-N-2-(N′-arginyl) aminoethyl ammonium chloride (DSAA), which could induce reactive oxygen species (ROS), inhibit MDR transporters, and enhance DOX uptake in NCI/ADR-RES cells; 2) a vascular endothelial growth factor (VEGF) siRNA, to increase DOX uptake and therapeutic efficacy via targeting tumor vasculature, disrupting local blood supply and blocking angiogenesis; 3) a therapeutic c-Myc siRNA, where the c-Myc is a well-known oncogene and shown to positively control the expression of MDR. Thus, the silencing of c-Myc may result in both a direct therapeutic effect and down-regulation of MDR.

2.2 Polymeric Nanoparticles

The Couvreur group entrapped DOX into biodegradable polyisobutylcyanoacrylate (PIBCA) polymers to form DOX-PIBCA NPs and showed the complete reversion of drug resistance *in-vitro* in several resistant cell lines [38]. The laser microspectrofluorometry technique was utilized to investigate the mechanisms of the NPs to overcome MDR. It was proposed that the DOX-PIBCA NPs entered the cells by endocytosis, and DOX was transported to the lysosomes and released close to the nuclear membrane, followed by interaction with DNA. It was also suggested that the DOX-PIBCA NPs bypassed the P-gp pump which was probably due to the molecular structure or the ionic charge of the NPs. Interestingly, this group suggested in another paper that the DOX-PIBCA NPs did not enter the cells by endocytosis pathway at all [39]. In contrast, the results demonstrated that the NPs were first adsorbed on the cell membrane, followed by the degradation of polymer close to cell membrane, and the drug was then released and entered the cells by simple passive diffusion. Compared to free DOX, the massive DOX concentration gradient from PIBCA NPs saturated P-gp and its pharmacological function. It was also suggested that PIBCA or its degradation products modified the cell membrane, which led to the permeation of more DOX into cells. In addition to NP-cell direct interaction, another mechanism was proposed wherein DOX formed ion pairs with the polyalkylcyanoacrylate (PACA) degradation product of polycyanoacrylic acid. This DOX-polycyanoacrylic acid ion-pair complex increased the apparent lipophilicity of DOX, and allowed the drug entering the cells bypass the recognition of P-gp. It was concluded that the reversal of MDR with DOX-PACA NPs was the result of both the adsorption of NPs on the cell surface and the formation of DOX-polycyanoacrylic acid ion-pair complex at the plasma membrane [40].

Henry-Toulmé et al. demonstrated that DOX-polyisohexylcyanoacrylate (DOX-PIHCA) NPs were not endocytosed by the cells, which supported the results from the Couvreur group [41]. Barraud and colleagues also developed DOX-PIHCA NPs and compared their antitumor efficacy versus free DOX both *in-vitro* and *in-vivo* in a resistant hepatocellular carcinoma (HCC) model [42]. The IC_{50} of NPs was reduced by 1.5–4.5-fold in *in-vitro* studies in several resistant HCC cells. *In-vivo* HCC transgenic mouse model, DOX-PIHCA NPs had significantly improved tumor inhibitory effect compared to free DOX ($p = 0.01$). The mechanisms by which DOX-PIHCA NPs bypass P-gp efflux were the same as DOX-PIBCA NPs discussed above. In similar, the Robert group prepared DOX-PIHCA NPs and showed complete reversal of MDR in resistant C6 0.001 cells [43]. It was found that only drug tightly associated with DOX-PIHCA NPs overcame P-gp resistance but empty NPs did not, while the empty liposomes alone blocked P-gp function, which indicated the different mechanisms to overcome P-gp resistance between the nano-delivery systems. It was also suggested that the mechanism by which DOX-PIHCA NPs bypassed P-gp rather than direct inhibit P-gp. In order to investigate whether free DOX or DOX-PIHCA NPs used different mechanisms to acquire MDR, two human tumor cell lines, K562 and MCF-7, were selected and DOX concentration in both formulations was gradually increased. It was found that DOX-PIHCA NPs were more difficult to generate resistant cell lines and P-gp expression was consistently lower than that in free DOX-selected cells, while breast cancer resistance protein (BCRP) expression was in a reverse order. These suggested different mechanisms may be involved in the acquisition of drug resistance [44]. Soma et al. prepared PACA NPs co-encapsulated of DOX and cyclosporine A (CyA, a P-gp inhibitor) and showed that the NPs had the most effective cell growth inhibition compared to other combinations of both drugs in solution or NPs with single drug alone in resistant P388/ADR cells [45, 46].

In addition to DOX-PACA NPs, Susa et al. successfully formulated DOX into a stearylamine-modified dextran NPs and demonstrated enhanced drug accumulation in the nucleus compared to free DOX in several resistant osteosarcoma cells [47]. It was found that the fluorescence of free DOX was mainly in the nucleus in sensitive cells but mainly in the

cytoplasm in resistant cells, while the drug distribution of NP formulation was mainly in the nucleus even in resistant cells. This indicated that the NP formulations were able to deliver DOX into the nucleus in resistant cells and the mechanisms may be due to bypassing of P-gp. Khdair et al. co-delivered DOX and methylene blue into Aerosol OT (AOT)-alginate NPs and this combination therapy significantly increased the *in-vitro* cytotoxicity in resistant NCI/ADR-RES cells and improved tumor growth inhibition *in-vivo* [48, 49]. Methylene blue is a photosensitizer and it is suggested to generate ROS and inhibit P-gp, although the mechanism is not fully understood [50]. It was hypothesized the P-gp inhibition and induced ROS of methylene blue increased the cytotoxicity of DOX in resistant cancer cells. Misra et al. also proposed dual drugs of DOX and curcumin co-encapsulated into poly(lactic-co-glycolic acid) (PLGA) NPs [51]. The application of curcumin helped the retention of DOX in the nucleus, as well as down-regulated the expression of P-gp and BCL-2 in K562 cells. The combination of both drugs in NP formulations had enhanced *in-vitro* cytotoxicity compared to single drug alone in either solution or NP formulations. Lei developed non-targeted and HER2 antibody conjugated DOX-loaded PLGA NPs and compared the cellular uptake and cytotoxicity to free DOX in resistant ovarian SKOV-3 and uterine MES-SA/Dx5 cells [52]. The results showed higher cellular uptake of targeted NPs than both of free drug or non-targeted NPs in SKOV-3 cells. It was suggested that the major mechanism of targeted PLGA NPs was receptor-mediated endocytosis. Shieh et al. developed more complex DOX NPs, where the chemotherapeutic agent DOX and a photosensitizer were co-incorporated into 4-armed porphyrin-polylactide (PPLA) NPs with D-α-tocopheryl polyethylene glycol 1000 succinate (TPGS, a P-gp inhibitor) coated on the NP surface [53]. It was concluded the combined agents showed a synergistic effect and increased DOX delivery to the nucleus in resistant MCF-7/ADR cells.

2.3 Polymeric Micelles

Alakhov et al. demonstrated that DNR-loaded poly(oxyethylene-b-oxypropylene-b-oxyethylene) (Pluronic P85) block copolymer micelles increased the cytotoxicity up to 3- and 700-fold greater than free DNR in sensitive SKOV3 and resistant SKVLB cells, respectively [54]. Based on the results from the cytotoxicity, influx and efflux, and drug-copolymer binding studies, it was hypothesized that the copolymer affected P-gp function by direct interaction with P-gp and/or changed the structure of the plasma membrane. In addition, the copolymer may induce the permeability of cell membrane. Lee et al. developed DOX-encapsulated poly(ethylene oxide)-poly(propylene oxide)-poly(ethylene oxide) (PEO-PPO-PEO) micelles and the micelle formulation exhibited 15-fold greater cytotoxicity compared to free DOX in MCF-7 cells [55]. The flow cytometry analysis and confocal images suggested the micelles entered the cells via the endocytosis pathway. Once inside cells, the micelles were initially localized in endosomes and DOX was then released in a sustained manner in the cytosol. The copolymer itself may also contribute to sensitization of cells and to the enhancement of DOX-induced cell apoptosis. Li and colleagues synthesized poly(L-lactide)-vitamin E TPGS (PLA-TPGS) block copolymer and used this as the carrier for DOX [56]. The results indicated that the PLA-TPGS micelles inhibited P-gp, enhanced drug cellular uptake, and facilitated translocation of DOX into the nucleus, all of which were responsible for MDR circumvention. Zhao and co-workers added TPGS into PLGA-PEG-folate polymeric micelles and showed increased DOX cellular uptake compared to the micelles without TPGS, which may be due to the P-gp inhibition of TPGS [57]. Other possible mechanisms of TPGS to overcome MDR may include inhibition of efflux pump ATPase and substrate binding, generation of ROS, and alteration of membrane fluidity [58–61]. Zheng et al. synthesized pH-sensitive polymers by linking N,N-diisopropylethylenediamine (DPA) onto the backbone of PEGylated polyphosphazene [62]. DOX was entrapped in the polymer to form self-assembled micelles and the IC_{50} value of this formulation was 60-fold lower than free DOX against resistant MCF-7/ADR cells. The

cellular uptake and intracellular distribution of DOX micelles were evaluated by confocal microscopy, and it was found that much more DOX was in the nucleus compared to free DOX and the majority of free DOX was entrapped in the intracellular compartments. Furthermore, DND-26 (an acidic organelle-selective fluorescent probe) was incorporated into the micelles to investigate whether the pH-sensitive polymeric micelles could help DOX escape from endosomes and lysosomes. The results demonstrated the fluorescence of DND-26 micelles was spread over the cells while free DND-26 was mainly located in the endosomes and lysosomes. Pre-incubation of the polymer solution followed by the addition of free DND-26 showed that the polymer and free DND-26 entered the cells via endocytosis and passive diffusion pathways, respectively. All these suggested the pH-sensitive polymeric micelles disrupted endosomes and released the drug after they were endocytosed into the cells, and that the mechanisms may be due to the proton-sponge effect and/or polymer-endosomal membrane interaction. Yuan et al. synthesized linoleic acid-grafted chitosan oligosaccharide (CSO-LA) and incorporated DOX into CSO-LA micelles [63, 64]. The results demonstrated a significant enhancement in the internalization of the micelles in both sensitive MCF-7 and K562 and their resistant cells compared to free DOX. In addition, paclitaxel (PX) and DOX were successfully co-loaded in the stearic acid-grafted CSO micelles and the results showed that this formulation was able to completely reverse MDR in resistant cells [65]. The following mechanisms were proposed for the fatty acid-grafted CSO micelles (CSO-FA) to overcome MDR: 1) positively-charged CSO-FA micelles facilitate the interaction between micelles and negatively-charged cell membrane; 2) the alkyl side chain on chitosan backbone favors its fusion and hydrophobic interactions with cell membrane and this effect was alkyl chain dependent; 3) the fatty acid forms hydrophobic microdomains near the surface of the micelle due to the stereo resistance effect, which enhances the hydrophobicity of the micelle and further favor the internalization of micelles into cells because of the lipophilic property of the cell membrane.

The Bae group developed DOX-loaded pH-sensitive polymeric micelles with folate (PHSM/f), which was a mixture of two block copolymers of poly(L-histidine)(M_n: 5K)-b-PEG (M_n: 2K) (polyHis/PEG) or polyHis/PEG with folate (polyHis/PEG-folate) and poly(L-lactic acid)(M_n: 3K)-b-PEG(M_n: 2K)-folate (pLLA/PEG-folate) [66–68]. The mixed copolymers in the micelle formulation improved the micelle stability in pH 7.4 due to the hydrophobic properties of pLLA [69]. This formulation overcame MDR both *in-vitro* and *in-vivo* in several resistant cell models. The results showed that the micelles entered the cells via folate receptor-mediated endocytosis pathway, and then DOX escaped from endosomes and was released into the cytoplasma due to the positively-charged polyHis which fused and destabilized the negatively-charged endosomal membrane at low pH of 6.5–7.2. To better understand the mechanism of the micelles, FITC-pLLA/PEG with folate (FITC-pLLA/PEG-folate) was synthesized as a pH-insensitive micelle control (PHIM/f). In contrast to PHSM/f, PHIM/f was found to be mostly entrapped into sub-organelles, such as endosomes, and had much less antitumor efficacy compared to PHSM/f. Taken together, the active folate receptor-mediated endocytosis, triggered drug release at low pH, and the interaction between polyHis group and endosomal membrane may be responsible for the MDR reversal effect. Later on, it was noticed that a fraction of the loaded DOX was released in tumor extracellular space (pH 6.5–7.2) before actively internalized into the cells. Therefore, the released drug had the potential to be pumped out by P-gp and attenuated its efficacy. To prevent DOX releasing in tumor extracellular space, L-phenylalanine (Phe) was introduced to the copolymer of polyHis/PEG to form poly(His-co-Phe)/PEG [70, 71]. The Phe group in the copolymers significantly dropped the pKa values and allowed the destabilization of micelles at even the lower pH of 6 to avoid the tumor extracellular pH. The mixture of poly(His-co-Phe)/PEG and pLLA/PEG-folate formed the second generation of pH-sensitive micelles which precisely target the early endosomes at pH of 6.

It has been shown that an NF- κB inhibitor enhanced tumor cell sensitivity of apoptosis induced by chemotherapeutic agents, such as DOX and PX [72, 73]. Fan et al. co-loaded DOX and pyrrolidinedithiocarbamate (PDTC, an NF- B inhibitor) in folate-chitosan (FA-CS) polymeric micelles, and the micelles showed significantly lower IC_{50} values and enhanced cellular uptake in resistant cells [74]. Lee et al. co-delivered human tumor necrosis factor (TNF)-related apoptosis-inducing ligand (Apo2L/TRAIL) and DOX with self-assembled micelles from cationic copolymer of poly{N-methyldietheneamine sebacate)-co-[(cholesteryl oxocarbonylamido ethyl) methyl bis(ethylene) ammonium bromide] sebacate} (P(MDS-co-CES)) [75]. It was demonstrated that the co-delivery of DOX and TRAIL in P(MDS-co-CES) micelles entered the cells via receptor-mediated endocytosis and enhanced the cytotoxicity against resistant tumor cells. Benoit et al. developed cationic micelles from copolymers of poly(dimethylaminoethyl methacrylate) (pDMAEMA) and poly(butyl methacrylate) (pDbB) [76]. DOX was loaded into the hydrophobic core of pDbB. An siRNA against polo-like kinase 1 (PLK1), a gene up-regulated in many cancers and responsible for cell cycle progression, was condensed with positively-charged pDMAEMA. A pH-sensitive copolymer of poly(styrene-alt-maleic anhydride) (pSMA) was further complexed with positively-charged PLK1 siRNA/DOX micelles to form a ternary complex for escape of the drug from endosomes. The co-delivery of PLK1 siRNA and DOX using this ternary complex system exhibited synergistic effect in resistant NCI/ADR-RES cells. Xiong et al. constructed poly(ethylene oxide)-block-poly(ε-caprolactone) (PEO-b-PCL) micelles for the co-delivery of MDR1 siRNA and DOX [77]. Two ligands, integrin αvβ3-specific ligand (RGD4C) and TAT peptide, were attached on the shell of the micelles for active targeting and cell-penetration purpose, respectively. This multifunctional polymeric micellar system was able to deliver both of DOX and MDR1 siRNA into intracellular compartments, and overcame P-gp-mediated resistance *in-vitro* and targeted αvβ3-positive tumors *in-vivo*. Nakanishi et al. prepared a polymeric micelle formulation of NK911 for DOX. NK911 consisted of block copolymers of PEG (M_w: 5K) and poly(aspartic acid) (~30 units) [78]. DOX was partially conjugated to the side chain of aspartic acid (~45%) to enhance the hydrophobicity of the inner core of the micelles. Therefore, two types of DOX, i.e. incorporated DOX and conjugated DOX, were in NK911 formulation. However, the conjugated DOX did not show any antitumor activity. The preclinical studies demonstrated much stronger tumor inhibitory effect against several tumor models compared to free DOX and currently NK911 is in a phase I trial.

In order to better understand the mechanism of polymeric micelle mediated drug delivery, Chen et al. investigated the cellular uptake of monomethoxy poly(ethylene glycol)-block-poly(D,L-lactic acid) (PEG-PDLLA) micelles [79]. Fluorescein isothiocyanate (FITC) was used to label micelle itself and 1,1′-dioctadecyl-3,3,3′,3′-tetramethylindocarbocyanine perchlorate ($DiIC_{18(3)}$) was used as a hydrophobic model molecule encapsulated in the micelle. It was found that the cellular uptake of $DiIC_{18(3)}$ was much faster than that of FITC-labeled PEG-PDLLA micelles, which indicated their different cell entry pathways. Moreover, förster resonance energy transfer (FRET) imaging and spectroscopy were utilized to monitor the cellular uptake of PEG-PDLLA micelles in real time loaded with a FRET pair of $DiIC_{18(3)}$ and 3,3′-dioctadecyloxacarbocyanine perchlorate ($DiOC_{18(3)}$). The FRET results confirmed that both of the hydrophobic dyes were entrapped in the core of the micelles and were subsequently released to the plasma membrane and then internalized by the cells. PEG on the shell of the micelles facilitated the release of the dyes because of the PEG-induced fusion to the cell membrane. In contrast, Allen et al. evaluated polycaprolactone-block-poly(ethylene oxide) (PCL_{20}-b-PEO_{44}) copolymer micelles in PC12 cells and the results strongly suggested the micelles entered the cells via endocytosis pathway based on a series of cellular uptake studies [80]. Savič et al. triple-labeled PCL-b-PEO micelles, nucleus, and plasma membrane (or cytoplasmic organelles, such as mitochondria, Golgi, etc.) and showed that the micelles were endocytosed into the cells and

distributed into several cytoplasmic compartments, including mitochondria, Golgi apparatus, but not the nucleus [81]. 5-dodecanoylaminofluorescein (DAF), a model molecule, was incorporated into PCL-b-PEO micelles and the results suggested the micelle formulation enhanced the delivery of the agent into the cells and increased its efficacy. Venne et al. demonstrated that the DOX-loaded poly(oxypropylene)-poly(oxyethylene) block copolymer pluronic L61 micelles enhanced by 290- and 700-fold the cytotoxicity in resistant CH^RC5 and MCF-7/ADR cells, respectively, but were comparable with free DOX in their matched sensitive cell lines [82]. The micelle formulation was found to shift the distribution of DOX from the cytoplasmic compartment to the nucleus, and the copolymer increased the drug uptake and inhibited the drug efflux. All of these contributed to the ability of pluronic L61 micelles to overcome MDR.

2.4 Polymer Conjugates

The Kopeček and Duncan groups collaboratively developed two N-(2-hydroxypropyl)methacrylamide (HPMA)-DOX conjugates, namely PK1 and PK2, and both of the conjugates were tested in phase I/II clinical trials [83]. The HPMA-DOX conjugates had the following three components: 1) a water-soluble polymeric carrier of HPMA; 2) an anticancer drug of DOX; 3) biodegradable polymer-drug linker. In the PK1 conjugate, the linker was a tetrapeptide of GFLG, which was stable in the blood circulation but susceptible to cleavage by enzymes in the lysosomes. In contrast, PK2 had additional galactose residues that were recognized by the asialoglycoprotein receptor on hepatocytes for targeted therapy of hepatocellular carcinoma. The IC_{50} value of HPMA-DOX conjugate in resistant A2780/AD cells was only about 20% higher than in sensitive A2780 cells (the resistance index of free DOX in A2780/AD cells: 40), which indicated that the conjugate formulation at least partially overcame P-gp-mediated resistance. The analysis of P-gp gene expression showed that free DOX at high doses induced P-gp expression in sensitive A2780 cell, while the HPMA-DOX conjugate inhibited P-gp and β_2-microglobulin (β_2m) genes in resistant A2780/AD cells.

The mechanisms of action of HPMA-DOX conjugates have been extensively studied and well established [84–89]. The HPMA-DOX conjugates entered the cells via endocytosis pathway and DOX was then released from the lysosomes in the perinuclear regions due to the lysosomally-degradable spacer of GFLG between DOX and the polymer. Then, the released DOX entered the nucleus and exerted its pharmacological function. The conjugates demonstrated prolonged blood circulation *in-vivo*, and enhanced tumor-to-blood ratio as a function of time, and enhanced C_{max} at 48 h in tumors after i.v. administration. All three of these parameters indicated that the conjugates passively accumulated in tumor tissues via the EPR effect. It is important to note that the particle size of HPMA-DOX conjugates was less than 10 nm. Interestingly, the concentration gradient of HPMA-DOX conjugates was found to be decreased from the perinuclear region to the plasma membrane. In contrast, the concentration gradient of free DOX was in the opposite direction, where it decreased from the plasma membrane to the perinuclear region. Consequently, DOX in the conjugate formulation had increased ability to interact with nuclear DNA and/or topoisomerase II. In addition, free DOX up-regulated MDR genes such as MDR1 and MRP, while the conjugates overcame MDR1 and down-regulated MRP. Free DOX also activated various cell detoxification mechanisms, while HPMA-DOX conjugate down-regulated BCL-2, heat-shock protein 70 (HSP-70), glutathione S-transferase π (GST-π), bilirubin uridine diphosphate (BUDP) transferases, topoisomerase IIα and IIβ, and thymidine kinase 1 (TK1) genes. With the exposure of HPMA-DOX conjugate, cell apoptosis, lipid peroxidation, and DNA damage were significantly higher compared to free DOX. For more details on the design, efficacy, safety, and mechanisms of action of HPMA-DOX conjugates, please refer to referenced articles [84–89].

Omelyanenko et al. synthesized targetable HPMA-DOX conjugates containing N-acylated galactosamine (GalN) or monoclonal OV-TL 16 antibodies (OV-TL 16 Ab) [90]. Fluorescence confocal microscopy studies demonstrated that both of the targeted conjugates had a similar fate when incubated with the cells, where the conjugates were recognized and internalized into the cells, localized in the lysosomes and DOX was then released from the polymer and eventually diffused from the cytoplasma into the nucleus. Šťastný et al. designed HPMA-DOX conjugates with different targeting moieties, including anti-CD71, antithymocyte globulin, anti-CD4, and transferrin, and compared their ability to reverse MDR in CEM/VLB cells [91]. Anti-CD4 targeted HPMA-DOX conjugate demonstrated the weakest ability to overcome resistance and this was probably due to the poor internalization of anti-CD4 molecule. It was hypothesized that receptor-mediated endocytosis was a very important factor for the MDR reversal effect of HPMA-DOX targeted conjugates and this effect was targeting moiety dependent. Nan et al. prepared targeted HPMA-DOX conjugates containing a peptide sequence of WHYPWFQNWAMA, to bind surface-specific receptor of Hsp47/CBP2 which was over-expressed in human squamous cell carcinoma of head and neck (SCCHN) [92]. Interestingly, both targeted and non-targeted conjugates demonstrated the less cellular uptake and lower cytotoxicity than free DOX in sensitive SCCHN cells. This indicated the endocytosis process of the conjugates was slower than the rapid passive diffusion of free DOX in sensitive SCCHN cells. In contrast, both targeted and non-targeted conjugates exhibited significantly higher cellular uptake and more potent than free DOX in resistant SCCHN cells. Moreover, targeted conjugates showed higher cellular uptake than non-targeted conjugates. Taken together, all the studies suggested the targeted HPMA-DOX conjugates had the potential to treat the resistant head and neck cancer. Bidwell et al. developed a thermally targeted elastin-like polypeptide (ELP) DOX conjugate to overcome MDR in resistant MES-SA/Dx5 and NCI/ADR-RES cells [93]. This DOX conjugate contained four functional domains: 1) an anticancer agent of DOX; 2) GFLG, a tetrapeptide linker, which could facilitate DOX release from lysosomes; 3) TAT, a cell penetrating peptide; 4) ELP, a thermal-responsive polypeptide as the vehicle for DOX. It was found to be beneficial to use ELP as a drug carrier compared to HPMA in PK1, based on the fact that ELP macromolecules accumulated in tumors and this accumulation may be further enhanced by thermal targeting.

In addition to HPMA-DOX conjugate, Kono et al. conjugated DOX to PEG modified poly(amidoamine) dendrimers with either an amide or hydrazone linkage [94]. The results demonstrated the acid-labile hydrazone linkage was very important to exhibit the antitumor efficacy in resistant cells. It was hypothesized the DOX-dendrimer conjugate was taken up into cells via endocytosis and entrapped into subcellular acidic compartments of endosomes and lysosomes. The endosomes were ruptured by DOX-dendrimer via proton sponge effect, and the hydrazone linkage was broken in acidic environment and DOX was then released from the dendrimer to exert its pharmacological action.

The Fong group applied a Schiff base covalent bond formation strategy to synthesize dextran-DOX conjugates [95–97]. Both free DOX and the conjugate were localized mainly in cytoplasmic compartments in resistant KB-V1 cells but for different reasons. Free DOX was difficult to diffuse into the nucleus due to the P-gp efflux, while the dextran-DOX conjugate was excluded from the nucleus due to its large size. The P-gp seemed to be only effective if the molecular weight of drug conjugates was less than 70 kDa. This was consistent with the findings that the central pore size of P-gp was 5 nm, while the effective size of 70 kDa dextran was ~5 nm [98]. Therefore, dextran-DOX conjugate larger than 70 kDa was not a good P-gp substrate and had better accumulation in the nucleus. Furthermore, the critical size of dextran for DOX accumulation was calculated as 103 kDa based on the relative cytotoxicity of dextran-DOX conjugate in sensitive and resistant KB cells. The DOX coupled to 70 kDa dextran, i.e. dextran-DOX conjugate (AD-70, DOX-OXD), was

tested in a phase I clinical trial and the MTD of the conjugate was found to be 40 mg DOX/m^2 [99].

2.5 Peptide/Protein Conjugates

Liang et al. synthesized a TAT-DOX conjugate and evaluated its cellular uptake and intracellular distribution in MCF-7 cells [100]. Both the conjugate and free DOX were transported into the cells but with different intracellular distribution, where free DOX was mainly in the nucleus while the most of the conjugate was located in the perinuclear and cytoplasmic regions. On the other hand, the cytotoxicity of the conjugate and free DOX was comparable. This suggested DOX also have activity in cytoplasma. The research supported that the activity of DOX was not only due to its inhibition of DNA synthesis, but also due to its interaction with cytoplasmic components to cause cell apoptosis [101]. Importantly, the cytotoxicity of the conjugate was about 8–10-fold higher than free DOX in both resistant MCF-7/ADR and AT3B-1 cells. To understand the mechanisms of TAT-DOX conjugate to overcome MDR, the intracellular DOX concentration was measured in sensitive and resistant MCF-7 cells. About 90% of the free DOX accumulated in sensitive cells but dropped to only 5% in resistant cells, indicating a strong P-gp efflux in resistant cells. In contrast, the conjugate had 58.6% retention in resistant cells. In addition, neither the mixture of DOX and TAT nor verapamil (a P-gp inhibitor) affected the cytotoxic properties of the TAT-DOX conjugate, which suggested the MDR reversal of the conjugate was bypassed but not inhibited. Aroui and colleagues designed three DOX-cell penetrating peptide (CPP) conjugates, namely maurocalcine, penetratin, and TAT, and compared the cytotoxicity to free DOX in different sensitive and resistant cells [102–104]. All three conjugates displayed similar efficacy which was about 5-fold more cytotoxic than free DOX in resistant cells. In general, CPPs are used as cell impermeable compounds, while the benefits of CPPs applied to the cell membrane permeable compound DOX may be due to improved stability, facilitated cell compartment targeting and DNA binding, alteration efflux pathways and detoxification reactions of DOX. To understand the mechanisms, BCL-2 and BCL-XL protein expressions were determined in the cells treated with DOX conjugates or free DOX since anti-apoptotic BCL-2 family was known to control mitochondria membrane permeability. However, the results showed no difference between the conjugate and free DOX. To determine if other apoptotic pathways were responsible for mitochondrial permeabilization, the DOX-CPP conjugates were studied in MDA-MB-231 cells over-expressing of BCL-2. It was found that the DOX conjugate was 5-fold more toxic than free DOX in resistant MDA-MB-231/BCL-2 cells, which indicated that the DOX-CPP conjugate activated multiple apoptotic pathways other than mitochondrial events. It should be noted that free DOX was mainly localized in the nucleus and the DOX conjugate was localized in the cytosol. The alteration of intracellular distribution of DOX conjugate may contribute the mitochondrial independent apoptotic pathways. Meyer-Losic et al. conjugated DOX to another CPP, Vectocell, via different linkers [105]. This peptide originated from human protein with 15–23 amino acid residues, and the studies showed it was internalized by different mechanisms [106]. When chemically stable bonds were utilized to the conjugate with Vectocell, e.g. at the C_{14} position of the thioether or the $C_{3'}$ position of the amide group of DOX, the *in-vivo* activity was minimal, which was probably due to inhibition of the interaction between DOX and DNA caused by Vectocell. The best linker was found to be at the C_{14} position of DOX with an ester bond, and this Vectocell-DOX conjugate had significantly greater antitumor efficacy compared to free DOX both *in-vitro* and *in-vivo* in colon and breast tumor models. The mechanism of the improved therapeutic index of Vectocell-DOX conjugate was not clear. However, because the conjugate had lower charge-to-mass ratio, it seemed to be different than other CPPs, such as TAT.

Mazel et al. coupled DOX to two different peptides, namely penetratin or SynB1, to obtain two different DOX-peptide conjugates [107]. The results demonstrated the IC_{50} value of the conjugates was about 20-fold less than free DOX in resistant K652/ADR cells, and the conjugates had similar cellular uptake in both sensitive and resistant cells. All of above results suggested that conjugate entered the resistant cells in a way not recognized by P-gp, although the mechanism was unknown. It was known that the amino group on DOX was an important substrate group for P-gp recognition and since the coupling of DOX to peptide was taken place at this amino position. Therefore, the conjugate may enter the resistant cells bypass of P-gp efflux. Interestingly, the cytotoxicity of the conjugate was less than that of free DOX in sensitive cells, indicating some loss of DOX activity which was probably due to the covalent binding between DOX and peptide. It should be noted that the conjugates in the studies were not susceptible to hydrolysis because succinate and thioether were used as the linkers for SynB1 and penetratin, respectively. When substituted succinate linker to disulfide, DOX-SynB1 conjugate was more potent. The DNA binding studies showed that the conjugate intercalated with DNA. Other mechanisms, such as interaction between conjugate and cell membrane, may be involved in the induction of the cell apoptosis by the conjugate.

Fritzer et al. synthesized transferrin-DOX conjugate and demonstrated that it was much more potent than free DOX in resistant K562/ADR, HL-60/ADR, KB-C1 and KB-V1 cells [108, 109]. Since a Schiff based coupling strategy was utilized to prepare transferrin-DOX conjugate, the conjugate did not undergo hydrolysis at acidic pH in the endocytic compartment. It was stable at least for 2 weeks at 37°C at pH 3.0 without detectable free DOX. The fluorescent microscope studies showed that the cell membrane, but not DNA, was the target of the conjugate. The mechanisms of transferrin-DOX conjugate were proposed where the conjugate slowly dissociated and released DOX in a sustained manner after binding to cell membrane, which prolonged the effect of DOX on cell membrane and caused membrane damage. In this way, P-gp was unable to circumvent the function of transferrin-DOX conjugate. In contrast, Lai et al. suggested a different mechanism of transferrin-DOX conjugate where the conjugate entered the cells and mainly localized in the cytoplasma [110]. It was pointed out that the discrepancy may be due to the different fluorescent labeling, where DOX fluorescence was quantified in Lai's studies while fluorescence-labeled transferrin was used for Fritzer's study. The increased cytotoxicity of transferrin-DOX conjugate over that of free DOX was partly explained by the conjugate bio-reductive processes and ROS generation in cytoplasma. The ability of the transferrin-DOX conjugate to overcome MDR was further confirmed by Łubgan, where the conjugate was 4- and 200-fold more cytotoxic than free DOX in sensitive HL-60 and resistant HL-60/ADR leukemia cells, respectively [111]. Interestingly, when Munns et al. investigated transferrin-DOX conjugate in sensitive MGH-U1 and resistant MGH-U1R bladder cancer cell lines, it was found that the conjugate did not overcome resistance [112]. It is worthy to mention that the mass spectrometry data demonstrated that the conjugate did not dissociate at all. To understand whether the integral conjugate form was active or not, transferrin-negative TRVb and transferrin-positive TRVb-1 cells were utilized as the controls. The results showed comparable cytotoxicity for the transferrin-DOX conjugate and free DOX, indicating that both of the DOX forms were equally active. It is known that the lipid composition and fluidity of cell membrane are different between resistant and sensitive cells, and this membrane acquired drug resistance may explain the transferrin-DOX conjugate failing to overcome resistance in MGH-U1R bladder cancer cells [113, 114].

Guillemard et al. linked DOX to a mAb specifically recognizing the type 1 insulin-like growth factor receptor (IGF-1R) [115]. This IGF-1R-DOX conjugate had more than a 200-fold enhanced therapeutic index compared to free DOX *in-vitro* in resistant KB-V cells, and significantly reduced the tumor burden *in-vivo* in a KB-V xenograft mouse model. Unlike

the transferrin-DOX conjugate, IGF-1R-DOX conjugate was internalized into cells via receptor-mediated endocytosis and DOX was released into the perinuclear and cytoplasmic regions farther away from the P-gp pump and therefore reducing the likelihood for efflux. Again, the amino group on DOX was used to couple with mAb. Therefore, this conjugate was able to escape P-gp recognition. Based on the fact that the luteinizing hormone-releasing hormone receptor (LHRH-R) is found in >50% of human breast cancers, Bajo et al. chemically coupled DOX to [D-Lys^6]LHRH to generate a cytotoxic conjugate, called AN-152 [116]. The AN-152 demonstrated significantly antitumor efficacy *in-vivo* compared to other controls in a DOX-resistant MX-1 xenograft mouse model. The following mechanisms of AN-152 were proposed to overcome resistance in MX-1 tumors: 1) AN-152 could significantly reduce HER2 and HER3 levels but not EGFR, while free DOX had no effect on these receptors. Therefore, down-regulation of ErbB/HER receptor family members may contribute to circumvent MDR; 2) the receptor-mediated endocytosis pathway of the conjugate via targeting to LHRH-R may not be the reason of its escape from the efflux pump because the resistance of DOX in MX-1 tumors is known not to be mediated by the transport system; 3) AN-152 significantly decreased mRNA levels of $G_{\alpha 11}$ and $G_{\alpha 12}$ but free DOX did not [117]. Both of the above G-proteins are known to couple to LHRH-R and regulate cell growth [118]. The disruption in G-protein signaling by AN-152 also contributed to circumvent MDR.

Ren et al. conjugated DOX to an antisense oligodeoxynucleotide (AS ODN, 5′-TCCTCCATTGCGGTCCCCTT-3′) on its 3′-phosphate group [119, 120]. The conjugate significantly enhanced the stability of both DOX and AS ODN in biological fluid *in-vitro*, and increased binding affinity of AS ODN to its complementary sequence. The intracellular accumulation of AS ODN was much higher in the conjugate form compared to free AS ODN, which was mainly due to the improved lipophilicity of AS ODN in conjugate. This AS ODN-DOX conjugate demonstrated significantly improved antitumor efficacy, and markedly inhibited P-gp expression and mRNA levels compared to AS ODN or DOX alone both *in-vitro* and *in-vivo* in a resistant KB-A-1 cell model.

The Ohkawa group developed a bovine serum albumin (BSA)-DOX conjugate and investigated the conjugate both *in-vitro* and *in-vivo* in sensitive AH66P and resistant AH66DR cells [121–124]. The results demonstrated the BSA-DOX conjugate had similar cytotoxicity *in-vitro* in both AH66P and AH66DR cells, which indicated the complete reversal of MDR (free DOX resistant index: 200). It was also found that DOX concentration in the cell remained relatively high even after 36 h. The treatment of BSA-DOX conjugate in rats in a resistant AH66DR model led to significantly prolonged survival compared to free DOX. All the results indicated this BSA-DOX conjugate had the potential to overcome MDR and it was suggested the conjugate entered the cells via endocytosis pathway and the drug was then slowly released from lysosomes. Furthermore, both of the drug concentration and molecular mass (M_r) of the internalized BSA-[^{14}C]DOX conjugate in different subcellular compartments (lysosomes, cytosol, nucleus, and mitochondria) were measured by a liquid scintillation counter and HPLC gel filtration, respectively. Interestingly, the accumulation of the conjugate markedly increased in lysosomes in resistant AH66DR cells as a function of time up to 24 h, while significantly enhanced accumulation in mitochondria but moderate increase in lysosomes and the nucleus was observed in sensitive AH66P cells. In both of the cell lines, a total of three peaks with M_r from 3–70 kDa were identified in lysosomes, one peak with M_r <2 kDa was in the nucleus and mitochondria, two peaks with one <2 kDa and the other one >500 kDa were determined in the cytosol. No free DOX was found in any compartments. The two peaks in the cytosol suggested that the smaller one (<2 kDa) may be the conjugate degradation product released from lysosomes, and the larger one (>500 kDa) may be the complex of the BSA-DOX conjugate or its degradation product with tubulin or other unknown proteins. It should be noted that the smaller peaks <2 kDa were

found in the nucleus, mitochondria and cytosol. In addition, based on the fact that the accumulation of the DOX BSA-[^{14}C]DOX conjugate increased in lysosomes in AH66DR cells, all of which indicated the BSA-DOX conjugate degraded in lysosomes and resultant active adducts <2 kDa were responsible for the antitumor efficacy in resistant AH66DR cells. To confirm the lysosomal degradation products from the conjugate exhibited cytotoxic effect, poly-D-lysine-DOX and poly-L-lysine-DOX conjugates were tested. The cellular uptake of both conjugate was similar, but only poly-L-lysine-DOX conjugate showed the cytotoxicity because poly-L-lysine was digested by lysosomal enzymes but poly-D-lysine did not [125]. Later on, four DOX-peptide conjugates with M_r <2 kDa, namely glycylglycine (diGly), glycylglycylglycine (triGly), reduced glutathione (GSH), and oxidized glutathione (GSSG), were synthesized and evaluated the cytotoxicity effect in both AH66P and AH66DR cells. diGly-DOX and triGly-DOX demonstrated the same cytotoxicity as free DOX in both of the cell lines, GSSG-DOX had the same cytotoxicity as BSA-DOX conjugate in both cells, and GSH-DOX showed 9- and 7.5-fold more cytotoxic activity than BSA-DOX conjugate against AH66P and AH66DR cells, respectively. The highest cytotoxicity of GSH-DOX among all DOX conjugates was due to the rapid uptake and high accumulation in resistant AH66DR cells.

2.6 Solid Lipid Nanoparticles

Kang et al. developed DOX-loaded solid lipid NPs (SLNs) with glyceryl caprate (Capmul MCM C10) as the lipid core, polyethylene glycol 660 hydroxystearate (Solutol HS15) as the surfactant, and curdlan as the shell forming material [126, 127]. The DOX SLNs enhanced the cellular uptake to 17.1- and 21.6-fold at 1 and 2 h, respectively, and increased apoptotic cell death determined by crystal violet staining assay, when compared to free DOX in resistant MCF-7/ADR cells. In addition, the SLNs did not induce hemolytic activity in human erythrocytes which indicated the safety of the formulation. It was concluded that the DOX SLNs had the potential to overcome MDR. The Mumper group successfully prepared DOX and IDA SLNs from warm microemulsion precursors using emulsifying wax as the oil phase, and polyoxyl 20-stearyl ether (Brij 78) and TPGS as the co-surfactants [128–132]. Anionic ion-paring agents of sodium taurodeoxycholate (STDC) and sodium tetradecyl sulfate (STS) were applied to neutralize the cationic anthracyclines and enhance the drug entrapment in SLNs. The DOX SLNs had significantly improved antitumor efficacy than free DOX both *in-vitro* and *in-vivo* in a resistant P388/ADR cell model, but IDA SLNs did not demonstrate any benefit compared to free IDA, which may be due to the more lipophilic property of IDA. The mechanisms of the DOX SLNs overcoming MDR were investigated and it was concluded that the MDR reversal of SLNs may due to the P-gp inhibition by Brij 78 and TPGS, and ATP depletion by Brij 78 [133]. It is known that SLNs have some potential limitations, such as low drug loading capacity, burst drug release behavior, and potential drug expulsion upon storage. To avoid the above limitations, the incorporation of liquid lipid to solid lipid, a second generation of SLN – nanostructured lipid carriers (NLC), was developed and found to enhance imperfections of SLNs and achieved more space for drug molecules, thus improved drug loading [134]. Zhang et al. applied monostearin as the solid lipid and oleic acid as the liquid lipid to construct DOX NLC [135]. This DOX NLC exhibited greater *in-vitro* cytotoxicity compared to free DOX in both resistant MCF-7/ADR and SKOV3-TR30 cells. The high affinity between lipids or NLC and the cell membrane, competitive inhibition of P-gp, all of above contributed the increased intracellular drug concentration and overcame MDR.

Wong et al. developed a novel polymer-lipid hybrid DOX SLN system which was composed of hydrolyzed polymer of epoxidized soybean oil (HPESO), stearic acid, pluronic F68, and DOX [136]. HPESO was applied not only to achieve more uniform and spherical particles, but also to enhance DOX partition in the SLN thereby increasing drug loading capacity. The

cytotoxicity of DOX SLNs was evaluated in resistant MDA435/LCC6/MDR1 cells, and the results showed SLNs were significantly more potent than free DOX. The mechanisms of DOX SLNs were investigated and proposed as the follows: 1) DOX is released from DOX SLNs outside the cells but the cytotoxicity is increased; 2) DOX-SLNs enter into the cells and DOX is then released from SLNs inside the cells, resulting in higher cytotoxicity. In the meanwhile, the following mechanisms were ruled out: 1) blank SLNs and/or excipients inhibit or bypass the MDR proteins based on the fact that the combination of blank SLNs and DOX or DOX-HPESO complex did not show significant cytotoxic effect in MDR cells; 2) the lipid components in the SLNs alter permeability of cell membrane. These two findings are quite different compared to nano-delivery systems discussed previously, which suggested the reversal of MDR activities was diversified and carrier dependent. Later, endocytosis inhibition and fluorescent image studies of SLNs were performed to better understand the mechanisms of the cellular drug uptake [137]. The results suggested the phagocytosis pathway was involved in SLN internalization and DOX associated with SLN bypassed the P-gp efflux in resistant cells. It was proposed that the DOX in SLNs probably entered the cells with the combination of simple passive diffusion of released drug from the carrier outside of cells and phagocytosis. The released drug outside of cells may in part be effluxed by P-gp, however, DOX that entered cells via phagocytosis would be entrapped in cells and difficult to be pumped out by P-gp. In another study, the co-delivery of DOX and GG918 (Elacridar, a lipophilic and non-ionic P-gp inhibitor) in the SLNs showed enhanced DOX cellular uptake than any forms of DOX/GG918 combination [138]. Shuhendler et al. developed polymer-lipid hybrid SLN with myristic acid, HPESO, pluronic F68, PEG100SA, PEG40SA, and both DOX and mitomycin C were simultaneously loaded in the SLNs [139]. The SLNs demonstrated to be 20–30-fold more toxic in resistant MB435/LCC6/MDR1 cells compared to free DOX.

2.7 Magnetic Nanoparticles

Chen et al. investigated how Fe_3O_4 magnetic NPs facilitated DNR to overcome MDR *in-vitro* in sensitive and resistant K562 cells [140]. To increase the interaction between NPs and lipid portion of cell membrane, tetraheptylammonium (THA) was coated on the NPs. Confocal fluorescence, atomic force microscope (AFM), and electrochemical studies were performed to evaluate the synergistic effects of NPs on the uptake of DNR in K562 cells. The observations confirmed the THA-coated Fe_3O_4 NPs interacted with cell membrane and significantly enhanced the uptake of DNR in resistant K562 cells. The similar size of THA capped Ni magnetic NPs were applied as a control, but the NPs showed much less efficacy in terms of DNR cellular uptake in both sensitive and resistant cells, indicating the unique property of THA capped Fe_3O_4 NPs to facilitate the DNR uptake. The following mechanisms were proposed for THA capped Fe_3O_4 NPs to overcome MDR: 1) Fe_3O_4 NPs may function as the inhibitor or competitive substrate for MDR associated proteins (e.g. P-gp); 2) the interaction between THA capped Fe_3O_4 NPs and cell membrane. Later on, both DOX and tetrandrine (Tet, a P-gp inhibitor) were loaded in Fe_3O_4 magnetic NPs and the results suggested the synergetic reversal effect in resistant K562/A02 cells [141]. Interestingly, Tet-Fe_3O_4 NPs were able to decrease by 100-fold the MDR1 mRNA level but could not reduce the total amount of P-gp, indicating P-gp function was blocked. The activity of a modified Tet, 5-bromotetrandrine (BrTet), was also evaluated and it was demonstrated to have better efficacy than Tet in resistant K562/A02 cells both *in-vitro* and *in-vivo* [142–145]. The BrTet-Fe_3O_4 NPs demonstrated the ability to down-regulate MDR1 mRNA level and P-gp expression. The combination of DNR and BrTet-Fe_3O_4 NPs also had significantly greater antitumor efficacy than any controls *in-vitro* in resistant K562/A02 cells and *in-vivo* in xenograft nude mice. It was confirmed this NP system inhibited BCL-2 expression, up-regulated BCL-2-associated X protein (BAX), p53 and caspase-3 proteins in resistant K562/A02 xenograft tumors, all of which contributed to synergetic effect of the

NPs to overcome MDR. Furthermore, short hairpin RNA (shRNA) targeted the sequences of 3491–3509, 1539–1557, and 3103–3121 nucleotide of MDR1 mRNA was constructed [146]. The *in-vitro* data suggested the combination of MDR1 shRNA and Fe_3O_4 magnetic NPs was more efficient to reverse MDR and less toxic in resistant K562/A02 cells. Similarly, DNR-loaded ZnO NPs were shown to have greater cytotoxicity compared to free DNR in resistant K562/A02 cells [147].

Kievit et al. developed a complex DOX NP formulation, where polyethylenimine (PEI)-DOX was first constructed via a pH-sensitive hydrazone linkage and this PEI-DOX was then conjugated to PEG-coated superparamagnetic iron oxide NPs [148]. PEI was used to serve as a docking molecule for DOX to achieve high drug loading and help it escape from endosomes. The results showed the complex NPs were rapidly taken up in both sensitive and resistant rat glioma C6 cells, and significantly enhanced drug retention and greater cytotoxicity compared to free DOX in resistant C6 cells. In addition, DOX had the fastest release profile at acidic pH, which indicated the cleavage of hydrazone linkage. Taken together, this DOX complex NPs overcame MDR *in-vitro*.

2.8 Gold Nanoparticles

Gold NPs (Au NPs) have been widely used as biomedical imaging and biosensors [149]. Because they are biocompatible, small size, high stability and tissue permeability, Au NPs are also served as effective drug delivery carriers and drugs could be associated on the NPs by physical adsorption, ionic bonding, and/or covalent bonding [150, 151]. Gu et al. conjugated DOX onto PEGylated Au NPs via a disulfide bond (Au-PEG-SS-DOX), and the NPs showed the greater intracellular drug uptake than free DOX in resistant HepG2-R cells, which was confirmed by both confocal images and inductively coupled plasma mass spectrometry (ICP-MS) [152]. Interestingly, the DOX was released from lysosomes and reached the cytoplasma but not the nucleus, which implied that the cytotoxic function of Au-PEG-SS-DOX was not through its interaction with nuclear DNA. It was suggested the ability of NPs to overcome MDR may be related to the cell membrane properties, and NPs may dysregulate mitochondrial function in cytoplasma thus inducing the cell apoptosis. Zhang et al. linked DOX onto Au NPs via an amide bond to form DOX-Au NPs with ultrasmall particle size of 2.7 nm [153]. The DOX-Au NPs were observed to be non-toxic and expected to be cleared by kidney within hours. The DOX-Au NPs were internalized into the cells and even entered into the nucleus as seen by confocal and electron microscopy, which was probably due to its small size. The NPs were demonstrated to have about 20- and 6-fold greater cytotoxicity and faster action than free DOX, respectively, in resistant B16 melanoma cells. The DOX-Au NPs were also sensitive to resistant HeLa cells over-expressing BCL-2, which was probably due to the entry of NPs into the nucleus and DNA damage caused by released DOX. The Fu group developed 3-mercaptopropionic acid capped Au NPs (MPA-capped Au NPs), and the NPs significantly facilitated DNR uptake compared to free DNR in resistant K562/ADM cells and the enhanced intracellular DNR fluorescence was mainly located on cell membrane [154, 155]. Interestingly, the Au NPs without MPA functional group did not show facilitated effect, suggesting this functional group played an important role in the enhanced DNR accumulation on cell membrane. It was suggested that MPA-capped Au NPs and free DNR formed a complex via electrostatic interaction thus facilitating drug penetration into the cells by simple diffusion and phagocytosis. Au NPs may also interact with proteins or other components on the cell membrane and circumvent MDR. Wang et al. conjugated DOX onto Au NPs via an acid-labile hydrazone linker (DOX-Au Hyd NPs) and NPs were confirmed to enter the cells via energy-dependent endocytosis, specifically, both caveolae- and clathrin-mediated endocytosis, and DOX was then released from the NPs to cytoplasma and the nucleus [156]. The DOX-Au Hyd NPs had significantly enhanced intracellular drug uptake and less efflux,

and dramatically increased cytotoxicity compared to free DOX in resistant MCF-7/ADR cells. DOX-Au NPs with a carbamate linker was prepared as a control (DOX-Au Cbm NPs) and the linkage was stable so that DOX was not released. In contrast, DOX-Au Cbm NPs demonstrated similar cytotoxicity as free DOX in MCF-7/ADR cells, indicating that the drug release from NPs was important to exert activity.

2.9 Silica Nanoparticles

Huang et al. covalently conjugated DOX onto mesoporous silica nanoparticles (MNSP) via hydrazone linkage (DOX Hyd MNSP) [157]. The DOX Hyd MNSP demonstrated significantly induced apoptosis both *in-vitro* and *in-vivo* in resistant MES-SA/Dx-5 cells compared to the controls. It was suggested the MNSP entered the cells via endocytosis and bypassed P-gp efflux pump. It was also claimed that this was the first report that MNSP overcame MDR *in-vivo*. Meng et al. engineered MNSP to simultaneously deliver DOX and MDR1 siRNA [158]. The surface of MNSP was functionalized with a phosphonate group which allowed DOX binding inside the MNSP via electrostatic action and this functional group coated with the cationic polymer of PEI which was further complexed with anionic MDR1 siRNA. The dual delivery of DOX and MDR1 siRNA with MNSP significantly enhanced intracellular and intranuclear DOX concentration compared to free DOX or DOX MNSP without siRNA in resistant KB-V1 cells. It was suggested that the DOX was released from lysosomes via proton sponge mechanism which was supported by the findings that the addition of NH_4Cl inhibited DOX release and entry into the nucleus. Shen et al. loaded DOX in MNSP and this DOX MNSP showed 8-fold more potent and dramatically enhanced drug intracellular uptake and nuclear accumulation than free DOX in resistant MCF-7/ADR cells *in-vitro* [159]. The DOX concentration of DOX MNSP was 6.12- and 5.11-fold greater than that of free DOX at 0.5 and 2 h, respectively, in xenograft MCF-7/ADR tumor-bearing nude mice. It was the first report that the MNSP itself inhibited P-gp expression based on its ability to down-regulate P-gp levels. The mechanism of MNSP entry into the cells was through micropinocytosis pathway and once the NPs internalized into the cell, MNSP may bypass P-gp because it was too large to be effluxed. All of the above probably contributed to the MNSP ability to overcome MDR. Chen et al. co-delivered DOX and BCL-2 siRNA in MNSP, where DOX was entrapped inside the pore of the MNSP and BCL-2 siRNA was complexed with MNSP modified polyamidoamine dendrimers [160]. The results demonstrated that the MNSPs enhanced drug cytotoxicity by up to 132-fold greater than that of free DOX in resistant A2780/AD human ovarian cancer cells, and that the significantly increased antitumor efficacy was probably due to the suppression of BCL-2 mRNA and perinuclear localization of DOX via MNSP delivery carrier.

2.10 Carbon Nanotubes

Li et al. coupled a P-gp antibody to functionalized carbon nanotubes via a diimide-activated amidation reaction for targeting purpose, and then loaded DOX on the remaining surface of the carbon nanotubes via physical adsorption [161]. The physical adsorption between DOX and nanotubes maximally preserved the molecule integrity because of the chemical bond avoidance. In addition, the release of DOX from nanotubes improved in a controlled manner upon exposure of DOX nanotubes under near-infrared radiation. It was proposed that the controllable and sustained release of DOX by near-infrared radiation and specific P-gp targeting were the main reasons that the nanotube overcame MDR in resistant human leukemia K562R cells. It was also suggested that the P-gp antibody conjugated on the nanotubes provided huge stereohindrance for P-gp recognition of DOX thus suppressed the efflux of DOX by P-gp.

2.11 Cyclodextrin Nanoparticles

Qiu and co-workers designed a delivery system of novel β-CD-centered star-shaped amphiphilic polymers (sPEL/CD) for DOX [162]. To construct the sPEL/CD complex, mPEG and PLA were reacted to form linear mPEG-PLA (mPEL) as the arms, and then β-CD served as the core to obtain sPEL/CD by an arm-first method. The drug loading of DOX was as high as 18% with an entrapment efficiency of 84%, which was probably due to the presence of PLA to increase hydrophobic interaction between polymer and drug as well as enlarge β-CD interspaces to accommodate more DOX. The DOX-loaded sPEL/CD had 3-fold decreased IC_{50} compared to free DOX in resistant MCF-7/ADR cells. Because it was reported that pluronic block copolymers were able to prevent MDR in cancer cells, it was hypothesized the mPEG-PLA block segment in sPEL/CD complex had similar effect due to its structural similarity to pluronic [163]. The interaction between polymer and P-gp may be another explanation of sPEL/CD system to reverse MDR.

3. Conclusions and Future Perspective

Anthracyclines are very effective chemotherapeutic drugs to treat various cancers. However, severe cardiotoxicity and the development of MDR are the major limitations for the application of anthracyclines in clinic.

Nano-delivery systems have emerged as the novel cancer therapeutics to overcome some of the limitations of anthracyclines. With the optimal particle sizes and surface properties, NPs may be able to passively target anthracyclines into the tumor tissues via the EPR effect, escape from RES recognition, prolong circulation time in blood, and improve the drug distribution in the body. Doxil, a DOX PEGylated liposome formulation, was approved in 1995. This formulation demonstrated slower plasma clearance, enhanced circulation and half-life, decreased cardiotoxicity compared to free DOX. However, it does not address MDR issue. To date, many nano-delivery systems have been developed and reported, such as liposome formulations, polymeric NPs, solid lipid NPs, mesoporous silica NPs, magnetic NPs, polymer-drug conjugates, to effectively circumvent MDR both *in-vitro* and *in-vivo*. Some of these systems have even been advanced to clinical trials, for example the HPMA-DOX conjugate. However, MDR is very complicated and multifactorial. In addition, the MDR mechanisms are not fully understood. Therefore, it is better to address different MDR pathways in the nano-delivery systems. For a given particular NP system, ideally it not only inhibits or bypasses efflux pump resistance, such as P-gp, BCRP and MRP1, but also circumvents non-pump resistance, such as BCL-2, p53, etc. Moreover, in addition to the passively targeting, the active targeting using ligands may further improve the anticancer efficacy in resistant tumors while decrease the toxicity in normal tissues.

Although nano-delivery systems are promising in cancer therapy, there remain many challenges for these systems. Notably, it is difficult to characterize nano-delivery systems *in-vivo*. As a consequence, there continues to be a lack of understanding of *in-vivo* NP stability and *in-vivo* drug release mechanisms. Also, the EPR effect is likely exaggerated in humans. However, nano-delivery systems with particle sizes as small as <40 nm may have a better chance to passively accumulate into tumors. Furthermore, the long-term toxicity of nano-materials is largely unknown. Nevertheless, the future of nano-delivery systems remains exciting and will certainly advance to address MDR in cancer therapy.

Acknowledgments

The authors are supported, in part, by Award Number U54 CA151652 from the National Cancer Institute. The content is solely the responsibility of the authors and does not necessarily represent the official views of the National Cancer Institute or the National Institutes of Health.

List of Abbreviations and Symbols

Ab	antibody
ABC	ATP-binding cassette
AFM	atomic force microscope
ALL	acute lymphocytic leukemia
AML	acute myeloid leukemia
AOT	Aerosol OT™
AS ODN	antisense oligodeoxynucleotide
ASO	antisense oligonucleotides
ATP	adenosine triphosphate
Au NPs	gold nanoparticles
AUC	area under the curve
BAX	BCL-2-associated X protein
BCL-2	B-cell lymphoma 2
BCRP	breast cancer resistance protein
Brij 78	polyoxyl 20-stearyl ether
BrTet	5-bromotetrandrine
BSA	bovine serum albumin
BUDP	bilirubin uridine diphosphate
Cbm	carbamate
CHOL	cholesterol
CL	cardiolipin
C_{max}	maximum concentration
c-Myc	v-myc myelocytomatosis viral oncogene homolog
CNT	carbon nanotubes
CPP	cell penetrating peptide
CSO	chitosan oligosaccharide
CyA	cyclosporine A
DAF	5-dodecanoylaminofluorescein
$DiIC_{18(3)}$	1,1′-dioctadecyl-3,3,3′,3′-tetramethylindocarbocyanine perchlorate
diGly	glycylglycine
$DiOC_{18(3)}$	3,3′-dioctadecyloxacarbocyanine perchlorate
DNA	deoxyribonucleic acid
DNR	daunorubicin
DOPA	1,2-dioleoyl-sn-glycero-3-phosphoethanolamine
DOTAP	N-[1-(2,3-dioleoyloxy)propyl]-N,N,N-trimethyl-ammonium methylsulfate

DOX	doxorubicin
DPA	N,N-diisopropylethylenediamine
DPPC	dipalmitoyl-phosphatidylcholine
DPPG	1,2-dipalmitoyl-sn-glycero-3-phosphoglycerol
DSAA	N,N-distearyl-N-methyl-N-2-(N′-arginyl) aminoethyl ammonium chloride
DSPC	1,2-distearoyl-sn-glycero-3-phosphocholine
EGFR	epidermal growth factor receptor
ELP	elastin-like polypeptide
EPC	egg phosphatidylcholine
EPR	enhanced permeability and retention
E-wax	emulsifying wax
FA	fatty acid
FA-CS	folate-chitosan
FITC	fluorescein isothiocyanate
FRET	förster resonance energy transfer
GalN	N-acylated galactosamine
GSH	reduced glutathione
GSSG	oxidized glutathione
GST	glutathione S-transferase
h	hour
HCC	hepatocellular carcinoma
HER2	human epidermal growth factor receptor 2
HIF1A	hypoxia-inducible factor 1α
HPESO	hydrolyzed polymer of epoxidized soybean oil
HPLC	high-performance liquid chromatography
HPMA	N-(2-hydroxypropyl)methacrylamide
HSP	heat-shock protein
IC_{50}	half maximal inhibitory concentration
ICP-MS	inductively coupled plasma mass spectrometry
IDA	idarubicin
IGF-1R	type 1 insulin-like growth factor receptor
i.v	intravenous
kg	kilogram
LA	linoleic acid
LHRH-R	luteinizing hormone-releasing hormone receptor

LPD	cationic liposome-polycation-DNA
LPD-II	anionic liposome-polycation-DNA
mAb	monoclonal antibody
MAL	maleimide
MDR	multiple drug resistance
mg	milligram
min	minute
mL	milliliter
MNSP	mesoporous silica nanoparticles
MPA	mercaptopropionic acid
mPEG	methoxy poly(ethylene glycol)
M_r	molecular mass
mRNA	messenger RNA
MRP	multidrug resistant protein
MTD	maximum tolerated dose
NC	nanocapsule
ng	nanogram
NLC	nanostructured lipid carriers
NP	nanoparticle
PACA	poly(alkyl cyanoacrylate)
PC	phosphatidylcholine
PCL	poly(ε-caprolactone)
PCL-b-PEO	polycaprolactone-block-poly(ethylene oxide)
pDbB	poly(butyl methacrylate)
PDLLA	poly(D,L-lactic acid)
pDMAEMA	poly(dimethylaminoethyl methacrylate)
PDTC	pyrrolidinedithiocarbamate
PEG	poly(ethylene glycol)
PEG-DSPE	polyethylene glycol-distearoylphosphatidylethanolamine
PEG-PDLLA	monomethoxy poly(ethylene glycol)-block-poly(D,L-lactic acid)
PEI	polyethylenimine
PEO-b-PCL	poly(ethylene oxide)-block-poly(ε-caprolactone)
PEO-PPO-PEO	poly(ethylene oxide)-poly(propylene oxide)-poly(ethylene oxide)
P-gp	P-glycoprotein
Phe	L-phenylalanine

PHIM/f	pH insensitive micelles with folate
PHSM/f	pH sensitive micelles with folate
PIBCA	polyisobutylcyanoacrylate
PIHCA	polyisohexylcyanoacrylate
PLA-TPGS	poly(L-lactide)-vitamin E TPGS
PLGA	poly(lactic-co-glycolic acid)
PLK1	polo-like kinase 1
pLLA/PEG	poly(L-lactic acid)-b-PEG
Pluronic P85	poly(oxyethylene-b-oxypropylene-b-oxyethylene)
P(MDS-co-CES)	poly{N-methyldietheneamine sebacate)-co-[(cholesteryl oxocarbonylamido ethyl) methyl bis(ethylene) ammonium bromide] sebacate}
p.o	per os
polyHis/PEG	poly(L-histidine)-b-PEG
PPLA	4-armed porphyrin-polylactide
pSMA	poly(styrene-alt-maleic anhydride)
PVA	poly(vinyl alcohol)
PX	paclitaxel
Ref	reference
RES	reticuloendothelial system
RGD4C	integrin αvβ3-specific ligand
RNA	ribonucleic acid
ROS	reactive oxygen species
SA	stearic acid
s.c	subcutaneous
SCCHN	squamous cell carcinoma of head and neck
shRNA	short hairpin RNA
siRNA	small interfering RNA
SLN	solid lipid nanoparticle
Solutol HS15	polyethylene glycol 660 hydroxystearate
STDC	sodium taurodeoxycholate
STS	sodium tetradecyl sulfate
$t_{1/2}$	half-life
Tet	tetrandrine
THA	tetraheptylammonium
TK1	thymidine kinase 1

TLC	thin layer chromatography
TNF	tumor necrosis factor
Topo	topoisomerase
TPGS	D-α-tocopheryl polyethylene glycol 1000 succinate
TRAIL	TNF-related apoptosis-inducing ligand
triGly	glycylglycylglycine
μg	microgram
μL	microliter
VEGF	vascular endothelial growth factor
VIP	vasoactive intestinal peptide
β_2m	β_2-microglobulin

References

1. Binaschi M, Bigioni M, Cipollone A, Rossi C, Goso C, Maggi CA, Capranico G, Animati F. Anthracyclines: selected new developments. Current Medicinal Chemistry Anti-Cancer Agents. 2001; 1:113–130. [PubMed: 12678762]
2. Minotti G, Menna P, Salvatorelli E, Cairo G, Gianni L. Anthracyclines: molecular advances and pharmacologic developments in antitumor activity and cardiotoxicity. Pharmacological Reviews. 2004; 56:185–229. [PubMed: 15169927]
3. Tan C, Tasaka H, Yu KP, Murphy ML, Karnofsk Da. Daunomycin, an antitumor antibiotic, in the treatment of neoplastic disease. Clinical evaluation with special reference to childhood leukemia. Cancer. 1967; 20:333–353. [PubMed: 4290058]
4. Arcamone F, Cassinelli G, Fantini G, Grein A, Orezzi P, Pol C, Spalla C. Adriamycin, 14-hydroxydaunomycin, a new antitumor antibiotic from S. peucetius var. caesius. Biotechnology and Bioengineering. 1969; 11:1101–1110. [PubMed: 5365804]
5. Arcamone F, Animati F, Capranico G, Lombardi P, Pratesi G, Manzini S, Supino R, Zunino F. New developments in antitumor anthracyclines. Pharmacology & Therapeutics. 1997; 76:117–124. [PubMed: 9535173]
6. Weiss RB. The anthracyclines: will we ever find a better doxorubicin. Semin Oncol. 1992; 19:670–686. [PubMed: 1462166]
7. Fields SM, Koeller JM. Idarubicin: a second-generation anthracycline. DICP: the Annals of Pharmacotherapy. 1991; 25:505–517. [PubMed: 2068836]
8. Goldenberg GJ, Wang H, Blair GW. Resistance to adriamycin: relationship of cytotoxicity to drug uptake and DNA single- and double-strand breakage in cloned cell lines of adriamycin-sensitive and -resistant P388 leukemia. Cancer Res. 1986; 46:2978–2983. [PubMed: 3698020]
9. Rhinehart JJ, Lewis RP, Balcerzak SP. Adriamycin cardiotoxicity in man. Ann Intern Med. 1974; 81:475–478. [PubMed: 4277990]
10. Lehne G. P-glycoprotein as a drug target in the treatment of multidrug resistant cancer. Current Drug Targets. 2000; 1:85–99. [PubMed: 11475537]
11. Kartner N, Riordan JR, Ling V. Cell surface P-glycoprotein associated with multidrug resistance in mammalian cell lines. Science. 1983; 221:1285–1288. [PubMed: 6137059]
12. Baekelandt MM, Holm R, Nesland JM, Tropé CG, Kristensen GB. P-glycoprotein expression is a marker for chemotherapy resistance and prognosis in advanced ovarian cancer. Anticancer Res. 2000; 20:1061–1067. [PubMed: 10810398]
13. Knoop AS, Knudsen H, Balslev E, Rasmussen BB, Overgaard J, Nielsen KV, Schonau A, Gunnarsdóttir K, Olsen KE, Mouridsen H, Ejlertsen B. Retrospective analysis of topoisomerase IIα amplifications and deletions as predictive markers in primary breast cancer patients randomly

assigned to cyclophosphamide, methotrexate, and fluorouracil or cyclophosphamide, epirubicin, and fluorouracil: Danish Breast Cancer Cooperative Group. J Clin Oncol. 2005; 23:7483–7490. [PubMed: 16234514]

14. Tanner M, Isola J, Wiklund T, Erikstein B, Kellokumpu-Lehtinen P, Malmström P, Wilking N, Nilsson J, Bergh J. Topoisomerase IIα gene amplification predicts favorable treatment response to tailored and dose-escalated anthracycline-based adjuvant chemotherapy in HER-2/neu-amplified breast cancer: Scandinavian Breast Group Trial 9401. J Clin Oncol. 2006; 24:2428–2436. [PubMed: 16682728]
15. Burger H, Foekens JA, Look MP, Meijer-van Gelder ME, Klijn JGM, Wiemer EAC, Stoter G, Nooter K. RNA expression of breast cancer resistance protein, lung resistance-related protein, multidrug resistance-associated proteins 1 and 2, and multidrug resistance gene 1 in breast cancer: correlation with chemotherapeutic response. Clinical Cancer Research. 2003; 9:827–836. [PubMed: 12576456]
16. Gottesman MM, Fojo T, Bates SE. Multidrug resistance in cancer: role of ATP-dependent transporters. Nat Rev Cancer. 2002; 2:48–58. [PubMed: 11902585]
17. Jain RK. Transport of molecules in the tumor interstitium: a review. Cancer Res. 1987; 47:3039–3051. [PubMed: 3555767]
18. Jain RK. Determinants of tumor blood flow: a review. Cancer Res. 1988; 48:2641–2658. [PubMed: 3282647]
19. Jain RK. Delivery of novel therapeutic agents in tumors: physiological barriers and strategies. J Natl Cancer Inst. 1989; 81:570–576. [PubMed: 2649688]
20. Hu CMJ, Zhang LF. Therapeutic nanoparticles to combat cancer drug resistance. Curr Drug Metab. 2009; 10:836–841. [PubMed: 20214578]
21. Jabr-Milane LS, van Vlerken LE, Yadav S, Amiji MM. Multi-functional nanocarriers to overcome tumor drug resistance. Cancer Treat Rev. 2008; 34:592–602. [PubMed: 18538481]
22. Maeda H, Wu J, Sawa T, Matsumura Y, Hori K. Tumor vascular permeability and the EPR effect in macromolecular therapeutics: a review. J Control Release. 2000; 65:271–284. [PubMed: 10699287]
23. Gabizon A, Martin F. Polyethylene glycol coated (pegylated) liposomal doxorubicin - rationale for use in solid tumours. Drugs. 1997; 54:15–21. [PubMed: 9361957]
24. Coukell AJ, Spencer CM. Polyethylene glycol-liposomal doxorubicin - a review of its pharmacodynamic and pharmacokinetic properties, and therapeutic efficacy in the management of AIDS-related Kaposi's sarcoma. Drugs. 1997; 53:520–538. [PubMed: 9074848]
25. Vail DM, Amantea MA, Colbern GT, Martin FJ, Hilger RA, Working PK. Pegylated liposomal doxorubicin: proof of principle using preclinical animal models and pharmacokinetic studies. Semin Oncol. 2004; 31:16–35. [PubMed: 15717736]
26. Thierry A, Vige D, Coughlin S, Belli J, Dritschilo A, Rahman A. Modulation of doxorubicin resistance in multidrug-resistant cells by liposomes. The FASEB Journal. 1993; 7:572–579.
27. Thierry AR, Dritschilo A, Rahman A. Effect of liposomes on P-glycoprotein function in multidrug resistant cells. Biochemical and Biophysical Research Communications. 1992; 187:1098–1105. [PubMed: 1356335]
28. Rahman A, Husain SR, Siddiqui J, Verma M, Agresti M, Center M, Safa AR, Glazer RI. Liposome-mediated modulation of multidrug resistance in human HL-60 leukemia cells. J Natl Cancer Inst. 1992; 84:1909–1915. [PubMed: 1361008]
29. Hu YP, Henrytoulme N, Robert J. Failure of liposomal encapsulation of doxorubicin to circumvent multidrug resistance in an in vitro model of rat glioblastoma cells. European Journal of Cancer. 1995; 31A:389–394. [PubMed: 7786607]
30. Riganti C, Voena C, Kopecka J, Corsetto PA, Montorfano G, Enrico E, Costamagna C, Rizzo AM, Ghigo D, Bosia A. Liposome-encapsulated doxorubicin reverses drug resistance by inhibiting P-glycoprotein in human cancer cells. Mol Pharm. 2011; 8:683–700. [PubMed: 21491921]
31. Krishna R, Mayer LD. Liposomal doxorubicin circumvents PSC 833-free drug interactions, resulting in effective therapy of multidrug-resistant solid tumors. Cancer Res. 1997; 57:5246–5253. [PubMed: 9393743]

32. Wang JC, Goh BC, Lu WL, Zhang Q, Chang A, Liu XY, Tan TMC, Lee HS. In vitro cytotoxicity of stealth liposomes co-encapsulating doxorubicin and verapamil on doxorubicin-resistant tumor cells. Biological & Pharmaceutical Bulletin. 2005; 8:822–828. [PubMed: 15863886]
33. Wu J, Lu YH, Lee A, Pan XG, Yang XJ, Zhao XB, Lee RJ. Reversal of multidrug resistance by transferrin-conjugated liposomes co-encapsulating doxorubicin and verapamil. J Pharm Pharm Sci. 2007; 10:350–357. [PubMed: 17727798]
34. Pakunlu RI, Wang Y, Saad M, Khandare JJ, Starovoytov V, Minko T. In vitro and in vivo intracellular liposomal delivery of antisense oligonucleotides and anticancer drug. J Control Release. 2006; 114:153–162. [PubMed: 16889867]
35. Wang Y, Saad M, Pakunlu RI, Khandare JJ, Garbuzenko OB, Vetcher AA, Soldatenkov VA, Pozharov VP, Minko T. Nonviral nanoscale-based delivery of antisense oligonucleotides targeted to hypoxia-inducible factor 1 alpha enhances the efficacy of chemotherapy in drug-resistant tumor. Clinical Cancer Research. 2008; 14:3607–3616. [PubMed: 18519795]
36. Saad M, Garbuzenko OB, Minko T. Co-delivery of siRNA and an anticancer drug for treatment of multidrug-resistant cancer. Nanomedicine. 2008; 3:761–776. [PubMed: 19025451]
37. Chen Y, Bathula SR, Li J, Huang L. Multifunctional nanoparticles delivering small interfering RNA and doxorubicin overcome drug resistance in cancer. J Biol Chem. 2010; 285:22639–22650. [PubMed: 20460382]
38. Cuvier C, Roblot-Treupel L, Millot JM, Lizard G, Chevillard S, Manfait M, Couvreur P, Poupon MF. Doxorubicin-loaded nanospheres bypass tumor cell multidrug resistance. Biochemical Pharmacology. 1992; 44:509–517. [PubMed: 1354963]
39. Verdière, ACd; Dubernet, C.; Nemati, F.; Poupon, MF.; Puisieux, F.; Couvreur, P. Uptake of doxorubicin from loaded nanoparticles in multidrug-resistant leukemic murine cells. Cancer Chemother Pharmacol. 1994; 33:504–508. [PubMed: 8137462]
40. deVerdiere AC, Dubernet C, Nemati F, Soma E, Appel M, Ferte J, Bernard S, Puisieux F, Couvreur P. Reversion of multidrug resistance with polyalkylcyanoacrylate nanoparticles: towards a mechanism of action. Br J Cancer. 1997; 76:198–205. [PubMed: 9231919]
41. Henry-Toulmé N, Grouselle M, Ramaseilles C. Multidrug resistance bypass in cells exposed to doxorubicin-loaded nanospheres: absence of endocytosis. Biochemical Pharmacology. 1995; 50:1135–1139. [PubMed: 7488226]
42. Barraud L, Merle P, Soma E, Lefrançois L, Guerret S, Chevallier M, Dubernet C, Couvreur P, Trépo C, Vitvitski L. Increase of doxorubicin sensitivity by doxorubicin-loading into nanoparticles for hepatocellular carcinoma cells in vitro and in vivo. Journal of Hepatology. 2005; 42:736–743. [PubMed: 15826724]
43. Bennis S, Chapey C, Couvreur P, Robert J. Enhanced cytotoxicity of doxorubicin encapsulated in polyisohexylcyanoacrylate nanospheres against multidrug-resistant tumour cells in culture. European Journal of Cancer. 1994; 30:89–93. [PubMed: 8142172]
44. Laurand A, Laroche-Clary A, Larrue A, Huet S, Soma E, Bonnet J, Robert J. Quantification of the expression of multidrug resistance-related genes in human tumour cell lines grown with free doxorubicin or doxorubicin encapsulated in polyisohexylcyanoacrylate nanospheres. Anticancer Res. 2004; 24:3781–3788. [PubMed: 15736412]
45. Emilienne Soma C, Dubernet C, Bentolila D, Benita S, Couvreur P. Reversion of multidrug resistance by co-encapsulation of doxorubicin and cyclosporin A in polyalkylcyanoacrylate nanoparticles. Biomaterials. 2000; 21:1–7. [PubMed: 10619673]
46. Soma CE, Dubernet C, Barratt G, Nemati F, Appel M, Benita S, Couvreur P. Ability of doxorubicin-loaded nanoparticles to overcome multidrug resistance of tumor cells after their capture by macrophages. Pharm Res. 1999; 16:1710–1716. [PubMed: 10571276]
47. Susa M, Iyer A, Ryu K, Hornicek F, Mankin H, Amiji M, Duan Z. Doxorubicin loaded polymeric nanoparticulate delivery system to overcome drug resistance in osteosarcoma. BMC Cancer. 2009; 9:399. [PubMed: 19917123]
48. Khdair A, Handa H, Mao G, Panyam J. Nanoparticle-mediated combination chemotherapy and photodynamic therapy overcomes tumor drug resistance in vitro. European Journal of Pharmaceutics and Biopharmaceutics. 2009; 71:214–222. [PubMed: 18796331]

49. Khdair A, Di C, Patil Y, Ma L, Dou QP, Shekhar MPV, Panyam J. Nanoparticle-mediated combination chemotherapy and photodynamic therapy overcomes tumor drug resistance. J Control Release. 2010; 141:137–144. [PubMed: 19751777]
50. Trindade GS, Farias SLA, Rumjanek VM, Capella MAM. Methylene blue reverts multidrug resistance: sensitivity of multidrug resistant cells to this dye and its photodynamic action. Cancer Letters. 2000; 151:161–167. [PubMed: 10738110]
51. Misra R, Sahoo SK. Coformulation of doxorubicin and curcumin in poly(D,L-lactide-co-glycolide) nanoparticles suppresses the development of multidrug resistance in K562 cells. Mol Pharm. 2011; 8:852–866. [PubMed: 21480667]
52. Lei T, Srinivasan S, Tang Y, Manchanda R, Nagesetti A, Fernandez-Fernandez A, McGoron AJ. Comparing cellular uptake and cytotoxicity of targeted drug carriers in cancer cell lines with different drug resistance mechanisms. Nanomedicine: Nanotechnology Biology and Medicine. 2011; 7:324–332.
53. Shieh MJ, Hsu CY, Huang LY, Chen HY, Huang FH, Lai PS. Reversal of doxorubicin-resistance by multifunctional nanoparticles in MCF-7/ADR cells. J Control Release. 2011; 152:418–425. [PubMed: 21435362]
54. Alakhov VY, Moskaleva EY, Batrakova EV, Kabanov AV. Hypersensitization of multidrug resistant human ovarian carcinoma cells by pluronic P85 block copolymer. Bioconjugate Chem. 1996; 7:209–216.
55. Lee Y, Park SY, Mok H, Park TG. Synthesis, characterization, antitumor activity of pluronic mimicking copolymer micelles conjugated with doxorubicin via acid-cleavable linkage. Bioconjugate Chem. 2007; 19:525–531.
56. Li PY, Lai PS, Hung WC, Syu WJ. Poly(L-lactide)-vitamin E TPGS nanoparticles enhanced the cytotoxicity of doxorubicin in drug-resistant MCF-7 breast cancer cells. Biomacromolecules. 2010; 11:2576–2582. [PubMed: 20722436]
57. Zhao H, Yung LYL. Addition of TPGS to folate-conjugated polymer micelles for selective tumor targeting. Journal of Biomedical Materials Research Part A. 2009; 91:505–518. [PubMed: 18985763]
58. Collnot EM, Baldes C, Wempe MF, Hyatt J, Navarro L, Edgar KJ, Schaefer UF, Lehr CM. Influence of vitamin E TPGS poly(ethylene glycol) chain length on apical efflux transporters in Caco-2 cell monolayers. J Control Release. 2006; 111:35–40. [PubMed: 16410030]
59. Yamagata T, Kusuhara H, Morishita M, Takayama K, Benameur H, Sugiyama Y. Effect of excipients on breast cancer resistance protein substrate uptake activity. J Control Release. 2007; 124:1–5. [PubMed: 17900739]
60. Collnot EM, Baldes C, Wempe MF, Kappl R, Hüttermann J, Hyatt JA, Edgar KJ, Schaefer UF, Lehr CM. Mechanism of inhibition of P-glycoprotein mediated efflux by vitamin E TPGS: influence on ATPase activity and membrane fluidity. Mol Pharm. 2007; 4:465–474. [PubMed: 17367162]
61. Mu L, Seow PH. Application of TPGS in polymeric nanoparticulate drug delivery system. Colloids and Surfaces B: Biointerfaces. 2006; 47:90–97.
62. Zheng C, Xu J, Yao X, Xu J, Qiu L. Polyphosphazene nanoparticles for cytoplasmic release of doxorubicin with improved cytotoxicity against Dox-resistant tumor cells. Journal of Colloid and Interface Science. 2011; 355:374–382. [PubMed: 21220138]
63. You J, Hu F, Du Y, Yuan H, Ye B. High cytotoxicity and resistant-cell reversal of novel paclitaxel loaded micelles by enhancing the molecular-target delivery of the drug. Nanotechnology. 2007; 18:495101–495107. [PubMed: 20442465]
64. Du Y, Wang L, Yuan H, Hu F. Linoleic acid-grafted chitosan oligosaccharide micelles for intracellular drug delivery and reverse drug resistance of tumor cells. International Journal of Biological Macromolecules. 2011; 48:215–222. [PubMed: 21093477]
65. Zhao M, Hu F, Du Y, Yuan H, Chen F, Lou Y, Yu H. Coadministration of glycolipid-like micelles loading cytotoxic drug with different action site for efficient cancer chemotherapy. Nanotechnology. 2009; 20:055102–055111. [PubMed: 19417333]
66. Lee ES, Na K, Bae YH. Doxorubicin loaded pH-sensitive polymeric micelles for reversal of resistant MCF-7 tumor. J Control Release. 2005; 103:405–418. [PubMed: 15763623]

67. Mohajer G, Lee E, Bae Y. Enhanced intercellular retention activity of novel pH-sensitive polymeric micelles in wild and multidrug resistant MCF-7 cells. Pharm Res. 2007; 24:1618–1627. [PubMed: 17385015]
68. Kim D, Lee E, Park K, Kwon I, Bae Y. Doxorubicin loaded pH-sensitive micelle: antitumoral efficacy against ovarian A2780/DOX^{R} tumor. Pharm Res. 2008; 25:2074–2082. [PubMed: 18449626]
69. Lee ES, Na K, Bae YH. Polymeric micelle for tumor pH and folate-mediated targeting. J Control Release. 2003; 91:103–113. [PubMed: 12932642]
70. Kim D, Lee ES, Oh KT, Gao ZG, Bae YH. Doxorubicin-loaded polymeric micelle overcomes multidrug resistance of cancer by double-targeting folate receptor and early endosomal pH. Small. 2008; 4:2043–2050. [PubMed: 18949788]
71. Kim D, Gao ZG, Lee ES, Bae YH. In vivo evaluation of doxorubicin-loaded polymeric micelles targeting folate receptors and early endosomal pH in drug-resistant ovarian cancer. Mol Pharm. 2009; 6:1353–1362. [PubMed: 19507896]
72. Nakanishi C, Toi M. Nuclear factor-[kappa]B inhibitors as sensitizers to anticancer drugs. Nat Rev Cancer. 2005; 5:297–309. [PubMed: 15803156]
73. Brantley E, Patel V, Stinson SF, Trapani V, Hose CD, Ciolino HP, Yeh GC, Gutkind JS, Sausville EA, Loaiza-Perez AI. The antitumor drug candidate 2-(4-amino-3-methylphenyl)-5-fluorobenzothiazole induces NF-kappa B activity in drug-sensitive MCF-7 cells. Anti-Cancer Drugs. 2005; 16:137–143. [PubMed: 15655410]
74. Fan L, Li F, Zhang H, Wang Y, Cheng C, Li X, Gu C-h, Yang Q, Wu H, Zhang S. Co-delivery of PDTC and doxorubicin by multifunctional micellar nanoparticles to achieve active targeted drug delivery and overcome multidrug resistance. Biomaterials. 2010; 31:5634–5642. [PubMed: 20430433]
75. Lee ALZ, Dhillon SHK, Wang Y, Pervaiz S, Fan W, Yang YY. Synergistic anti-cancer effects via co-delivery of TNF-related apoptosis-inducing ligand (TRAIL/Apo2L) and doxorubicin using micellar nanoparticles. Molecular BioSystems. 2011; 7:1512–1522. [PubMed: 21350763]
76. Benoit DSW, Henry SM, Shubin AD, Hoffman AS, Stayton PS. pH-responsive polymeric sirna carriers sensitize multidrug resistant ovarian cancer cells to doxorubicin via knockdown of polo-like kinase 1. Mol Pharm. 2010; 7:442–455. [PubMed: 20073508]
77. Xiong XB, Lavasanifar A. Traceable multifunctional micellar nanocarriers for cancer-targeted co-delivery of MDR-1 siRNA and doxorubicin. ACS Nano. 2011; 5:5202–5213. [PubMed: 21627074]
78. Nakanishi T, Fukushima S, Okamoto K, Suzuki M, Matsumura Y, Yokoyama M, Okano T, Sakurai Y, Kataoka K. Development of the polymer micelle carrier system for doxorubicin. J Control Release. 2001; 74:295–302. [PubMed: 11489509]
79. Chen H, Kim S, Li L, Wang S, Park K, Cheng JX. Release of hydrophobic molecules from polymer micelles into cell membranes revealed by Förster resonance energy transfer imaging. Proceedings of the National Academy of Sciences. 2008; 105:6596–6601.
80. Allen C, Yu Y, Eisenberg A, Maysinger D. Cellular internalization of PCL20-b-PEO44 block copolymer micelles. Biochimica et Biophysica Acta (BBA) -Biomembranes. 1999; 1421:32–38.
81. Savić R, Luo L, Eisenberg A, Maysinger D. Micellar nanocontainers distribute to defined cytoplasmic organelles. Science. 2003; 300:615–618. [PubMed: 12714738]
82. Venne A, Li S, Mandeville R, Kabanov A, Alakhov V. Hypersensitizing effect of pluronic L61 on cytotoxic activity, transport, and subcellular distribution of doxorubicin in multiple drug-resistant cells. Cancer Res. 1996; 56:3626–3629. [PubMed: 8705995]
83. Minko T, Kopecková P, Pozharov V, Kopecek J. HPMA copolymer bound adriamycin overcomes MDR1 gene encoded resistance in a human ovarian carcinoma cell line. J Control Release. 1998; 54:223–233. [PubMed: 9724909]
84. Kopecek J, Kopecková P, Minko T, Lu ZR. HPMA copolymer-anticancer drug conjugates: design, activity, and mechanism of action. European Journal of Pharmaceutics and Biopharmaceutics. 2000; 50:61–81. [PubMed: 10840193]
85. Kopecek J, Kopecková P. HPMA copolymers: origins, early developments, present, and future. Advanced Drug Delivery Reviews. 2010; 62:122–149. [PubMed: 19919846]

86. Duncan R. Designing polymer conjugates as lysosomotropic nanomedicines. Biochem Soc Trans. 2007; 35:56–60. [PubMed: 17233601]
87. Sirova M, Mrkvan T, Etrych T, Chytil P, Rossmann P, Ibrahimova M, Kovar L, Ulbrich K, Rihova B. Preclinical evaluation of linear HPMA-doxorubicin conjugates with pH-sensitive drug release: efficacy, safety, and immunomodulating activity in murine model. Pharm Res. 2010; 27:200–208. [PubMed: 19894105]
88. Minko T. HPMA copolymers for modulating cellular signaling and overcoming multidrug resistance. Advanced Drug Delivery Reviews. 2010; 62:192–202. [PubMed: 20005272]
89. Ríhová B, Kovár M. Immunogenicity and immunomodulatory properties of HPMA-based polymers. Advanced Drug Delivery Reviews. 2010; 62:184–191. [PubMed: 19914318]
90. Omelyanenko V, Kopeková P, Gentry C, Kopeek J. Targetable HPMA copolymer-adriamycin conjugates. Recognition, internalization, and subcellular fate. J Control Release. 1998; 53:25–37. [PubMed: 9741911]
91. St'astný M, Strohalm J, Plocová D, Ulbrich K, Ríhová B. A Possibility to overcome P-glycoprotein (PGP)-mediated multidrug resistance by antibody-targeted drugs conjugated to N-(2-hydroxypropyl)methacrylamide (HPMA) copolymer carrier. European Journal of Cancer. 1999; 35:459–466. [PubMed: 10448300]
92. Nan A, Ghandehari H, Hebert C, Siavash H, Nikitakis N, Reynolds M, Sauk JJ. Water-soluble polymers for targeted drug delivery to human squamous carcinoma of head and neck. J Drug Target. 2005; 13:189–197. [PubMed: 16036307]
93. Bidwell G, Davis A, Fokt I, Priebe W, Raucher D. A thermally targeted elastin-like polypeptide-doxorubicin conjugate overcomes drug resistance. Invest New Drugs. 2007; 25:313–326. [PubMed: 17483874]
94. Kono K, Kojima C, Hayashi N, Nishisaka E, Kiura K, Watarai S, Harada A. Preparation and cytotoxic activity of poly(ethylene glycol)-modified poly(amidoamine) dendrimers bearing adriamycin. Biomaterials. 2008; 29:1664–1675. [PubMed: 18194811]
95. Fong WF, Lam W, Yang MS, Wong JTF. Partial synergism between dextran-conjugated doxorubicin and cancer drugs on the killing of multidrug resistant KB-V1 cells. Anticancer Res. 1996; 16:3773–3778. [PubMed: 9042256]
96. Lam W, Chan HL, Yang MS, Cheng SK, Fong WF. Synergism of energy starvation and dextran-conjugated doxorubicin in the killing of multidrug-resistant KB carcinoma cells. Anti-Cancer Drugs. 1999; 10:171–178. [PubMed: 10211547]
97. Lam W, Leung CH, Chan HL, Fong WF. Toxicity and DNA binding of dextran-doxorubicin conjugates in multidrug-resistant KB-V1 cells: optimization of dextran size. Anti-Cancer Drugs. 2000; 11:377–384. [PubMed: 10912954]
98. Rosenberg MF, Callaghan R, Ford RC, Higgins CF. Structure of the multidrug resistance P-glycoprotein to 2.5 nm resolution determined by electron microscopy and image analysis. J Biol Chem. 1997; 272:10685–10694. [PubMed: 9099718]
99. Danhauser-Riedl S, Hausmann E, Schick HD, Bender R, Dietzfelbinger H, Rastetter J, Hanauske AR. Phase I clinical and pharmacokinetic trial of dextran conjugated doxorubicin (AD-70, DOX-OXD). Invest New Drugs. 1993; 11:187–195. [PubMed: 7505268]
100. Liang JF, Yang VC. Synthesis of doxorubicin-peptide conjugate with multidrug resistant tumor cell killing activity. Bioorg Med Chem Lett. 2005; 15:5071–5075. [PubMed: 16168650]
101. Mizutani H, Tada-Oikawa S, Hiraku Y, Kojima M, Kawanishi S. Mechanism of apoptosis induced by doxorubicin through the generation of hydrogen peroxide. Life Sciences. 2005; 76:1439–1453. [PubMed: 15680309]
102. Aroui S, Brahim S, De Waard M, Bréard J, Kenani A. Efficient induction of apoptosis by doxorubicin coupled to cell-penetrating peptides compared to unconjugated doxorubicin in the human breast cancer cell line MDA-MB 231. Cancer Letters. 2009; 285:28–38. [PubMed: 19523755]
103. Aroui S, Ram N, Appaix F, Ronjat M, Kenani A, Pirollet F, De Waard M. Maurocalcine as a non toxic drug carrier overcomes doxorubicin resistance in the cancer cell line MDA-MB 231. Pharm Res. 2009; 26:836–845. [PubMed: 19083085]

104. Aroui S, Brahim S, Waard MD, Kenani A. Cytotoxicity, intracellular distribution and uptake of doxorubicin and doxorubicin coupled to cell-penetrating peptides in different cell lines: a comparative study. Biochemical and Biophysical Research Communications. 2010; 391:419–425. [PubMed: 19914216]

105. Meyer-Losic F, Quinonero J, Dubois V, Alluis B, Dechambre M, Michel M, Cailler F, Fernandez AM, Trouet A, Kearsey J. Improved therapeutic efficacy of doxorubicin through conjugation with a novel peptide drug delivery technology (Vectocell). J Med Chem. 2006; 49:6908–6916. [PubMed: 17154520]

106. De Coupade C, Fittipaldi A, Chagnas V, Michel M, Carlier S, Tasciotti E, Darmon A, Ravel D, Kearsey J, Giacca M, Cailler F. Novel human-derived cell-penetrating peptides for specific subcellular delivery of therapeutic biomolecules. Biochem J. 2005; 390:407–418. [PubMed: 15859953]

107. Mazel M, Clair P, Rousselle C, Vidal P, Scherrmann JM, Mathieu D, Temsamani J. Doxorubicin-peptide conjugates overcome multidrug resistance. Anti-Cancer Drugs. 2001; 12:107–116. [PubMed: 11261883]

108. Fritzer M, Barabas K, Szüts V, Berczi A, Szekeres T, Faulk WP, Goldenberg H. Cytotoxicity of a transferrin-adriamycin conjugate to anthracycline-resistant cells. International Journal of Cancer. 1992; 52:619–623.

109. Fritzer M, Szekeres T, Szüts V, Jarayam HN, Goldenberg H. Cytotoxic effects of a doxorubicin-transferrin conjugate in multidrug-resistant KB cells. Biochemical Pharmacology. 1996; 51:489–493. [PubMed: 8619895]

110. Lai BT, Gao JP, Lanks KW. Mechanism of action and spectrum of cell lines sensitive to a doxorubicin-transferrin conjugate. Cancer Chemother Pharmacol. 1998; 41:155–160. [PubMed: 9443629]

111. Łubgan D, JoŸwiak Z, Grabenbauer G, Distel L. Doxorubicin-transferrin conjugate selectively overcomes multidrug resistance in leukaemia cells. Cellular and Molecular Biology Letters. 2009; 14:113–127. [PubMed: 18850074]

112. Munns J, Yaxley J, Coomer J, Lavin MF, Gardiner RA, Watters D. Evaluation of the potential of transferrin-adriamycin conjugates in the treatment of bladder cancer. Br J Urol. 1998; 82:284–289. [PubMed: 9722768]

113. Vrignaud P, Montaudon D, Londos-Gagliardi D, Robert J. Fatty acid composition transport and metabolism in doxorubicin-sensitive and-resistant rat glioblastoma cells. Cancer Res. 1986; 46:3258–3261. [PubMed: 3708560]

114. Tarasiuk J, Garnier-Suillerot A. Kinetic parameters for the uptake of anthracycline by drug-resistant and drug-sensitive K562 cells. European Journal of Biochemistry. 1992; 204:693–698. [PubMed: 1541282]

115. Guillemard V, Uri Saragovi H. Prodrug chemotherapeutics bypass p-glycoprotein resistance and kill tumors in vivo with high efficacy and target-dependent selectivity. Oncogene. 2004; 23:3613–3621. [PubMed: 15034547]

116. Bajo AM, Schally AV, Halmos G, Nagy A. Targeted doxorubicin-containing luteinizing hormone-releasing hormone analogue AN-152 inhibits the growth of doxorubicin-resistant MX-1 human breast cancers. Clinical Cancer Research. 2003; 9:3742–3748. [PubMed: 14506166]

117. Arcamone F, Animati F, Berettoni M, Bigioni M, Cipollone A, Franciotti M, Lombardi P, Madami A, Manzini S, Salvatore C, Capranico G, Caserini C, De Cesare M, Polizzi D, Pratesi G, Righetti SC, Supino R, Zunino F, Casazza AM. Doxorubicin disaccharide analogue: apoptosis-related improvement of efficacy in vivo. J Natl Cancer Inst. 1997; 89:1217–1223. [PubMed: 9274917]

118. Dhanasekaran N, Tsim ST, Dermott JM, Onesime D. Regulation of cell proliferation by G proteins. Oncogene. 1998; 17:1383–1394. [PubMed: 9779986]

119. Ren Y, Wei D, Zhan X. Inhibition of P-glycoprotein and increasing of drug-sensitivity of a human carcinoma cell line (KB-A-1) by an antisense oligodeoxynucleotide-doxorubicin conjugate in vitro. Biotechnology and Applied Biochemistry. 2005; 41:137–143. [PubMed: 15202936]

120. Ren Y, Wang Y, Zhang Y, Wei D. Overcoming multidrug resistance in human carcinoma cells by an antisense oligodeoxynucleotide-doxorubicin conjugate in vitro and in vivo. Mol Pharm. 2008; 5:579–587. [PubMed: 18461970]

121. Ohkawa K, Hatano T, Tsukada Y, Matsuda M. Chemotherapeutic efficacy of the protein-doxorubicin conjugates on multidrug resistant rat hepatoma cell line in vitro. Br J Cancer. 1993; 67:274–278. [PubMed: 8431358]

122. Ohkawa K, Hatano T, Yamada K, Joh K, Takada K, Tsukada Y, Matsuda M. Bovine serum albumin-doxorubicin conjugate overcomes multidrug resistance in a rat hepatoma. Cancer Res. 1993; 53:4238–4242. [PubMed: 8364920]

123. Takahashi N, Asakura T, Ohkawa K. Pharmacokinetic analysis of protein-conjugated doxorubicin (DXR) and its degraded adducts in DXR-sensitive and -resistant rat hepatoma cells. Anti-Cancer Drugs. 1996; 7:687–696. [PubMed: 8913438]

124. Asakura T, Takahashi N, Takada K, Inoue T, Ohkawa K. Drug conjugate of doxorubicin with glutathione is a potent reverser of multidrug resistance in rat hepatoma cells. Anti-Cancer Drugs. 1997; 8:199–203. [PubMed: 9073316]

125. Shen W, Ryser H. Poly (L-lysine) and poly (D-lysine) conjugates of methotrexate: different inhibitory effect on drug resistant cells. Molecular Pharmacology. 1979; 16:614–622. [PubMed: 514261]

126. Subedi RK, Kang KW, Choi HK. Preparation and characterization of solid lipid nanoparticles loaded with doxorubicin. European Journal of Pharmaceutical Sciences. 2009; 37:508–513. [PubMed: 19406231]

127. Kang KW, Chun MK, Kim O, Subedi RK, Ahn S-G, Yoon J-H, Choi H-K. Doxorubicin-loaded solid lipid nanoparticles to overcome multidrug resistance in cancer therapy. Nanomedicine: Nanotechnology Biology and Medicine. 2010; 6:210–213.

128. Ma P, Dong X, Swadley CL, Gupte A, Leggas M, Ledebur HC, Mumper RJ. Development of idarubicin and doxorubicin solid lipid nanoparticles to overcome Pgp-mediated multiple drug resistance in leukemia. J Biomed Nanotechnol. 2009; 5:151–161. [PubMed: 20055093]

129. Ma P, Benhabbour SR, Feng L, Mumper RJ. 2′-Behenoyl-paclitaxel conjugate containing lipid nanoparticles for the treatment of metastatic breast cancer. Cancer Letters. (In Press).

130. Holpuch A, Hummel G, Tong M, Seghi G, Pei P, Ma P, Mumper R, Mallery S. Nanoparticles for local drug delivery to the oral mucosa: proof of principle studies. Pharm Res. 2010; 27:1224–1236. [PubMed: 20354767]

131. Ma P, Mumper RJ. Paclitaxel nano-delivery systems: a comprehensive review. Journal of Nanomedicine and Nanotechnology. 2013; 4:164.

132. Feng L, Wu H, Ma P, Mumper RJ, Benhabbour SR. Development and optimization of oil-filled lipid nanoparticles containing docetaxel conjugates designed to control the drug release rate in vitro and in vivo. Int J Nanomedicine. 2011; 6:2545–2556. [PubMed: 22072889]

133. Dong X, Mattingly CA, Tseng MT, Cho MJ, Liu Y, Adams VR, Mumper RJ. Doxorubicin and paclitaxel-loaded lipid-based nanoparticles overcome multidrug resistance by inhibiting P-glycoprotein and depleting ATP. Cancer Res. 2009; 69:3918–3926. [PubMed: 19383919]

134. Müller RH, Radtke M, Wissing SA. Nanostructured lipid matrices for improved microencapsulation of drugs. Int J Pharm. 2002; 242:121–128. [PubMed: 12176234]

135. Zhang XG, Miao J, Dai YQ, Du YZ, Yuan H, Hu FQ. Reversal activity of nanostructured lipid carriers loading cytotoxic drug in multi-drug resistant cancer cells. Int J Pharm. 2008; 361:239–244. [PubMed: 18586075]

136. Wong HL, Rauth AM, Bendayan R, Manias J, Ramaswamy M, Liu Z, Erhan S, Wu XY. A new polymer-lipid hybrid nanoparticle system increases cytotoxicity of doxorubicin against multidrug-resistant human breast cancer cells. Pharm Res. 2006; 23:1574–1585. [PubMed: 16786442]

137. Wong HL, Bendayan R, Rauth AM, Xue HY, Babakhanian K, Wu XY. A mechanistic study of enhanced doxorubicin uptake and retention in multidrug resistant breast cancer cells using a polymer-lipid hybrid nanoparticle system. J Pharmacol Exp Ther. 2006; 317:1372–1381. [PubMed: 16547167]

138. Wong HL, Bendayan R, Rauth AM, Wu XY. Simultaneous delivery of doxorubicin and GG918 (Elacridar) by new polymer-lipid hybrid nanoparticles (PLN) for enhanced treatment of multidrug-resistant breast cancer. J Control Release. 2006; 116:275–284. [PubMed: 17097178]
139. Shuhendler A, Cheung R, Manias J, Connor A, Rauth A, Wu X. A novel doxorubicin-mitomycin C co-encapsulated nanoparticle formulation exhibits anti-cancer synergy in multidrug resistant human breast cancer cells. Breast Cancer Res Treat. 2010; 119:255–269. [PubMed: 19221875]
140. Wang X, Zhang R, Wu C, Dai Y, Song M, Gutmann S, Gao F, Lv G, Li J, Li X, Guan Z, Fu D, Chen B. The application of Fe_3O_4 nanoparticles in cancer research: a new strategy to inhibit drug resistance. Journal of Biomedical Materials Research Part A. 2007; 80:852–860. [PubMed: 17072850]
141. Chen BA, Sun Q, Wang XM, Gao F, Dai YY, Yin Y, Ding JJ, Gao C, Cheng J, Li JJ, Sun XC, Chen NN, Xu WL, Shen HL, Liu DL. Reversal in multidrug resistance by magnetic nanoparticle of Fe_3O_4 loaded with adriamycin and tetrandrine in K562/A02 leukemic cells. Int J Nanomed. 2008; 3:277–286.
142. Wang J, Chen B, Cheng J, Xu W, Sun X. Comparison of reversal effects of 5-bromotetrandrine and tetrandrine on P-glycoprotein-dependent resistance to adriamycin in human lukemia cell line K562/A02. Chinese Journal of Cancer. 2008; 27:491–495. [PubMed: 18479598]
143. Cheng J, Wu WW, Chen BA, Gao F, Xu WL, Gao C, Ding JH, Sun YY, Song HH, Bao W, Sun XC, Xu CR, Chen WJ, Chen NN, Liu LJ, Xia GH, Li XM, Wang XM. Effect of magnetic nanoparticles of Fe_3O_4 and 5-bromotetrandrine on reversal of multidrug resistance in K562/A02 leukemic cells. Int J Nanomed. 2009; 4:209–216.
144. Chen BA, Cheng J, Shen MF, Gao F, Xu WL, Shen HL, Ding JH, Gao C, Sun Q, Sun XC, Cheng HY, Li GH, Chen WJ, Chen NN, Liu LJ, Li XM, Wang XM. Magnetic nanoparticle of Fe_3O_4 and 5-bromotetrandrin interact synergistically to induce apoptosis by daunorubicin in leukemia cells. Int J Nanomed. 2009; 4:65–71.
145. Chen BA, Cheng J, Wu YA, Gao F, Xu WL, Shen HL, Ding JH, Gao C, Sun Q, Sun XC, Cheng HY, Li GH, Chen WJ, Chen NN, Liu LJ, Li XM, Wang XM. Reversal of multidrug resistance by magnetic Fe_3O_4 nanoparticle copolymerizating daunorubicin and 5-bromotetrandrine in xenograft nude-mice. Int J Nanomed. 2009; 4:73–78.
146. Chen BA, Mao PP, Cheng JA, Gao F, Xia GH, Xu WL, Shen HL, Ding JH, Gao C, Sun QA, Chen WJ, Chen NN, Liu LJ, Li XM, Wang XM. Reversal of multidrug resistance by magnetic Fe_3O_4 nanoparticle copolymerizating daunorubicin and MDR1 shRNA expression vector in leukemia cells. Int J Nanomed. 2010; 5:437–444.
147. Guo D, Wu C, Jiang H, Li Q, Wang X, Chen B. Synergistic cytotoxic effect of different sized ZnO nanoparticles and daunorubicin against leukemia cancer cells under UV irradiation. Journal of Photochemistry and Photobiology B: Biology. 2008; 93:119–126.
148. Kievit FM, Wang FY, Fang C, Mok H, Wang K, Silber JR, Ellenbogen RG, Zhang M. Doxorubicin loaded iron oxide nanoparticles overcome multidrug resistance in cancer in vitro. J Control Release. 2011; 152:76–83. [PubMed: 21277920]
149. Yu AM, Liang ZJ, Cho JH, Caruso F. Nanostructured electrochemical sensor based on dense gold nanoparticle films. Nano Letters. 2003; 3:1203–1207.
150. Chen YH, Tsai CY, Huang PY, Chang MY, Cheng PC, Chou CH, Chen DH, Wang CR, Shiau AL, Wu CL. Methotrexate conjugated to gold nanoparticles inhibits tumor growth in a syngeneic lung tumor model. Mol Pharm. 2007; 4:713–722. [PubMed: 17708653]
151. Podsiadlo P, Sinani VA, Bahng JH, Kam NWS, Lee J, Kotov NA. Gold nanoparticles enhance the anti-leukemia action of a 6-mercaptopurine chemotherapeutic agent. Langmuir. 2007; 24:568–574. [PubMed: 18052300]
152. Gu YJ, Cheng J, Man CWY, Wong WT, Cheng SH. Gold-doxorubicin nanoconjugates for overcoming multidrug resistance, Nanomedicine: Nanotechnology. Biology and Medicine. 2012; 8:204–211.
153. Zhang X, Chibli H, Mielke R, Nadeau J. Ultrasmall gold-doxorubicin conjugates rapidly kill apoptosis-resistant cancer cells. Bioconjugate Chem. 2010; 22:235–243.

154. Song M, Wang X, Li J, Zhang R, Chen B, Fu D. Effect of surface chemistry modification of functional gold nanoparticles on the drug accumulation of cancer cells. Journal of Biomedical Materials Research Part A. 2008; 86:942–946. [PubMed: 18067157]

155. Li J, Wang X, Wang C, Chen B, Dai Y, Zhang R, Song M, Lv G, Fu D. The enhancement effect of gold nanoparticles in drug delivery and as biomarkers of drug-resistant cancer cells. ChemMedChem. 2007; 2:374–378. [PubMed: 17206735]

156. Wang F, Wang YC, Dou S, Xiong MH, Sun TM, Wang J. Doxorubicin-tethered responsive gold nanoparticles facilitate intracellular drug delivery for overcoming multidrug resistance in cancer cells. ACS Nano. 2011; 5:3679–3692. [PubMed: 21462992]

157. Huang IP, Sun SP, Cheng SH, Lee CH, Wu CY, Yang CS, Lo LW, Lai YK. Enhanced chemotherapy of cancer using pH-sensitive mesoporous silica nanoparticles to antagonize P-glycoprotein-mediated drug resistance. Molecular Cancer Therapeutics. 2011; 10:761–769. [PubMed: 21411714]

158. Meng H, Liong M, Xia T, Li Z, Ji Z, Zink JI, Nel AE. Engineered design of mesoporous silica nanoparticles to deliver doxorubicin and P-glycoprotein siRNA to overcome drug resistance in a cancer cell line. ACS Nano. 2010; 4:4539–4550. [PubMed: 20731437]

159. Shen J, He Q, Gao Y, Shi J, Li Y. Mesoporous silica nanoparticles loading doxorubicin reverse multidrug resistance: performance and mechanism. Nanoscale. 2011

160. Chen AM, Zhang M, Wei D, Stueber D, Taratula O, Minko T, He H. Co-delivery of doxorubicin and Bcl-2 siRNA by mesoporous silica nanoparticles enhances the efficacy of chemotherapy in multidrug-resistant cancer cells. Small. 2009; 5:2673–2677. [PubMed: 19780069]

161. Li R, Wu R, Zhao L, Wu M, Yang L, Zou H. P-glycoprotein antibody functionalized carbon nanotube overcomes the multidrug resistance of human leukemia cells. ACS Nano. 2010; 4:1399–1408. [PubMed: 20148593]

162. Qiu LY, Wang RJ, Zheng C, Jin Y, Jin LQ. β-cyclodextrin-centered star-shaped amphiphilic polymers for doxorubicin delivery. Nanomedicine. 2010; 5:193–208. [PubMed: 20148632]

163. Batrakova EV, Kelly DL, Li S, Li Y, Yang Z, Xiao L, Alakhova DY, Sherman S, Alakhov VY, Kabanov AV. Alteration of genomic responses to doxorubicin and prevention of MDR in breast cancer cells by a polymer excipient: pluronic P85. Mol Pharm. 2005; 3:113–123. [PubMed: 16579640]

Biographies

Ping Ma received his B.S. degree in Pharmaceutics in 2000 from China Pharmaceutical University, Nanjing, China. Ma earned his M.S. degree in Industrial Pharmacy in 2006 from the University of Toledo, Toledo, OH. Subsequently, he began his Ph.D. studies in Dr. Russell J. Mumper’s laboratory and received a Ph.D. degree in Pharmaceutics in 2012 from the University of North Carolina at Chapel Hill with a focus on the development of lipid-based nanoparticle formulations for improved cancer treatment. Currently, Dr. Ma is working for Hospira Inc.

Russell J. Mumper is the Vice Dean and the John A. McNeill Distinguished Professor at the UNC Eshelman School of Pharmacy at the University of North Carolina (UNC) at Chapel Hill. Dr. Mumper has 25 years of experience in the pharmaceutical/ biotechnology industries and academia with expertise in advanced drug delivery systems and product development and commercialization. Dr. Mumper received his Ph.D. in Pharmaceutics/Drug Delivery and a B.A. in Chemistry from the University of Kentucky, Lexington, KY.

Highlights

- The most comprehensive review to discuss anthracycline nano-delivery systems to overcome multiple drug resistance (MDR).
- More than ten types of developed anthracycline nano-delivery systems to overcome MDR are discussed.
- More than ten proposed cellular mechanisms of developed anthracycline nano-delivery systems to overcome MDR are discussed.
- Provides a useful guidance for further nanoparticle formulation development to overcome MDR.

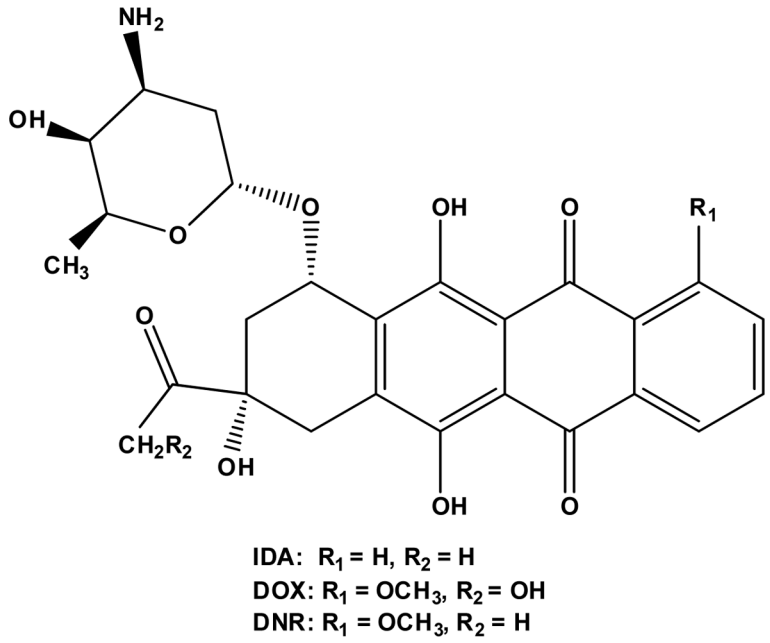

Figure 1.
Chemical Structures of DOX, DNR and IDA.

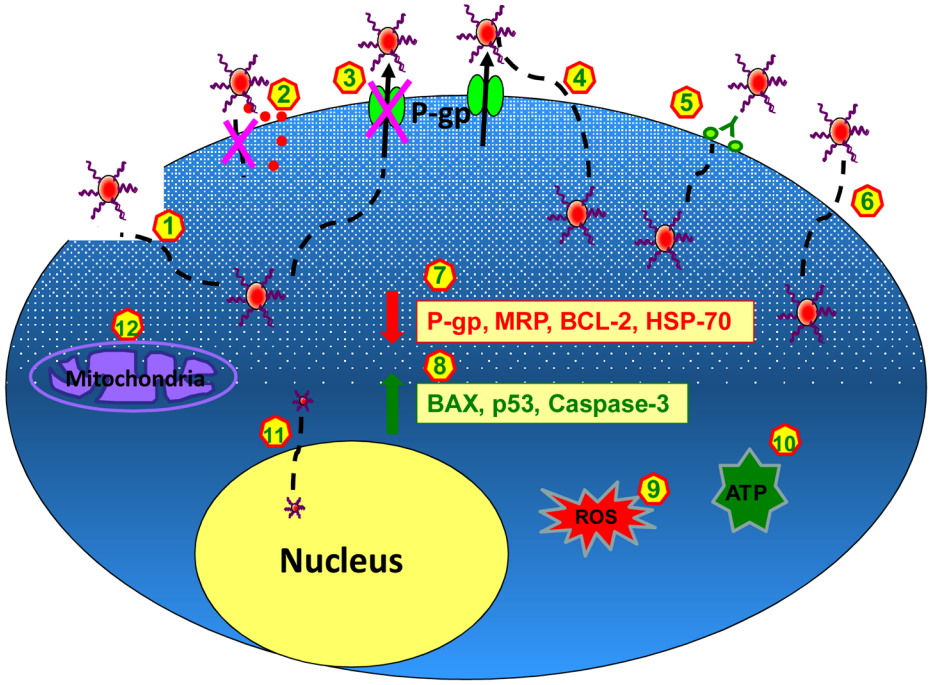

Figure 2. Summary of the Proposed Cellular Mechanisms of Anthracycline NPs to Overcome MDR

(1) NPs interact with or modify plasma membrane and therefore change the membrane structure and induce membrane permeability; (2) NPs do not enter cells; instead free drugs are released to plasma membrane and then diffuse into cells; (3) NPs directly interact with and inhibit P-gp; (4) NPs bypass, but do not inhibit P-gp; (5) NPs enter into cells via receptor-mediated endocytosis; (6) NPs enter into cells via endocytosis, phagocytosis, or micropinocytosis; (7) NPs down-regulate P-gp, MRP, BCL-2, and HSP-70; (8) NPs up-regulate BAX, p53, and caspase-3; (9) NPs generate ROS; (10) NPs deplete ATP; (11) Very small NPs enter into the nucleus; (12) NPs dysregulate mitochondrial function or activate mitochondrial independent apoptotic pathways.

Table 1

Physicochemical Properties of DOX, DNR, and IDA.

	DOX	DNR	IDA
Formula	$C_{27}H_{29}NO_{11}$	$C_{27}H_{29}NO_{10}$	$C_{26}H_{27}NO_9$
Molecular Weight (g/mol)	543.52	527.52	497.49
Water Solubility (mg/mL)	92.8	39.2	35.6
Log P	1.27	1.68	2.10
pKa	~8.4	10.3	8.5
Melting Point (°C)	204–205	208–209	173–174
Half-life (h)	55	18.5	22
Protein Binding (%)	70	97	97

Table 2

Summary of the Proposed Mechanisms of Anthracycline NPs to Overcome MDR.

Platform	Composition	Mechanism	Status	Ref.
Liposome	CL, PC, CHOL	interact with P-gp modify plasma membrane	*in-vitro*	[27, 28]
	CL, PC, CHOL	increase drug accumulation intracellular drug redistribution	*in-vitro*	[26]
	DSPE-PEG, CHOL, DPPC, DPPG	direct inhibit ATPase alter raft lipid composition reduce lipid raft-associated P-gp	*in-vitro*	[30]
	DSPC, CHOL	PSC 833 (P-gp inhibitor)	*in-vivo*	[31]
	EPC, CHOL, PEG- DSPE	verapamil (P-gp inhibitor)	*in-vitro*	[32]
	EPC, CHOL, mPEG-DSPE, MAL-PEG-DSPE	verapamil (P-gp inhibitor) transferrin (targeting)	*in-vitro*	[33]
	EPC, CHOL, DSPE-PEG, DPPC	MDR1 ASO BCL-2 ASO endocytosis membrane fusion	*in-vivo*	[34]
	DOTAP	MRP1 siRNA BCL-2 siRNA	*in-vitro*	[36]
	DSAA, DOTAP, DOPA, CHOL, DSPE-PEG, DSPE-PEG-AA	DSAA (induce ROS, inhibit MDR transporters, enhance drug uptake) VEGF siRNA (increase drug uptake and targeting) c-Myc siRNA (improve therapeutic effect and down- regulate MDR)	*in-vivo*	[37]
Polymeric NP	PIBCA	PIBCA and its degradation products change or modify cell membrane massive drug diffusion from NPs saturates P-gp NPs do not enter the cells	*in-vitro*	[39]
	PACA	NP-cell interaction on cell surface form drug-polycyanoacrylic acid ion-pair complex cyclosporine A (P-gp inhibitor)	*in-vitro*	[40, 45, 46]
	PIHCA	bypass but not direct inhibit P-gp	*in-vitro*	[42, 43]
	AOT-alginate	methylene blue (inhibit P-gp and generate ROS)	*in-vitro*	[48, 49]
	PPLA	porphyrin (photosensitizer) TPGS (P-gp inhibitor)	*in-vitro*	[53]
	stearyl-modified dextran	bypass P-gp	*in-vitro*	[47]
	PLAG	curcumin (increase drug retention in the nucleus; down-regulate P-gp and BCL-2)	*in-vitro*	[51]
	PLGA	receptor-mediated endocytosis (HER2)	*in-vitro*	[52]
Polymeric Micelles	pluronic P85	interact with P-gp change cell membrane structure induce cell membrane permeability	*in-vitro*	[54]
	PEO-PPO-PEO	endocytosis sensitize cells	*in-vitro*	[55]
	PLA-TPGS	inhibit P-gp enhance drug cellular uptake promote drug to translocate into the nucleus	*in-vitro*	[56]
	PLGA-PEG-folate	TPGS (P-gp inhibitor)	*in-vitro*	[57]
	PEG- polyphosphazene	endocytosis	*in-vitro*	[62]

Platform	Composition	Mechanism	Status	Ref.
		pH-sensitive polymer (disrupt endosomes by proton- sponge effect and/or interact between polymer and endosome membrane)		
	CSO-FA	interact with cell membrane alkyl side chain on chitosan introduces perturbation effect fatty acids form hydrophobic microdomains near shell surface	*in-vitro*	[63–65]
	polyHis/PEG (or polyHis/PEG-folate), pLLA/PEG- folate	receptor-mediated endocytosis (folate) trigger drug release at low pH (pH-sensitive) interact between polyHis group of the micelle and endosome membrane	*in-vivo*	[66–69]
	PEO-b-PCL	RGD4C (targeting) TAT (cell-penetration peptide) MDR1 siRNA	*in-vivo*	[77]
	PEG-PDLLA	drug released to plasma membrane and then internalized into cells PEG-induced fusion to cell membrane	*in-vitro*	[79]
	PCL-PEO	endocytosis	*in-vitro*	[80, 81]
	pluronic L61	facilitate drug entry into the nucleus increase drug cellular uptake inhibit drug efflux	*in-vitro*	[82]
Polymer Conjugate	HPMA	inhibit P-gp and β_2m lysosomally degradable linker (GFLG) endocytosis down-regulate P-gp, MRP, BCL-2, HSP-70, etc.	*phase I/II*	[83–89]
	dextran	endocytosis bypass P-gp	*phase I*	[95–97]
	PEG-modified dendrimer	endocytosis rupture endosomes (proton-sponge effect)	*in-vitro*	[94]
Magnetic NP	Fe_3O_4, ZnO	P-gp inhibitor or competitive P-gp substrate (Fe_3O_4) interact between NPs and cell membrane tetrandrine (P-gp inhibitor) up-regulate BAX, p53, caspase-3 inhibit BCL-2, down-regulate P-gp shRNA (targeting)	*in-vivo*	[140–147]
Carbon Nanotube	—	controllable and sustained drug release P-gp antibody (targeting)	*in-vitro*	[161]
CD NP	—	interaction between polymer and P-gp inhibit P-gp	*in-vitro*	[162]
Peptide/ Protein Conjugate	TAT	bypass but not inhibit P-gp	*in-vitro*	[100, 101]
	maurocalcine, penetratin, TAT	active mitochondrial independent apoptotic pathways	*in-vitro*	[102–104]
	Vectocell	internalization	*in-vitro*	[105, 106]
	penetratin, SynB1	bypass P-gp interact between conjugate and cell membrane	*in-vitro*	[107]
	transferrin	bypass P-gp (conjugate slowly dissociates after binding to cell membrane) receptor-mediated endocytosis interact between conjugate and DNA	*in-vitro*	[108, 109]
	IGF-1R mAb	receptor-mediated endocytosis escape P-gp recognition	*in-vivo*	[115]
	[D-Lys^6]LHRH	not by receptor-mediated endocytosis down-regulate ErbB/HER receptors disrupt G-protein signaling	*in-vivo*	[116–118]

Platform	Composition	Mechanism	Status	Ref.
	AS-ODN	high drug accumulation inhibit P-gp (AS-ODN)	*in-vivo*	[119, 120]
	BSA	endocytosis conjugate degrades in lysosomes	*in-vivo*	[121–123]
	diGly, triGly, GSH, GSSG	rapid drug uptake high drug accumulation	*in-vitro*	[124]
	poly-D-Lysine, poly-L-Lysine	endocytosis poly-L-Lysine digested by lysosomes	*in-vitro*	[125]
SLNs	emulsifying wax, Brij 78, TPGS	inhibit P-gp, deplete ATP, increase drug retention	*in-vivo*	[128, 133]
	monostearin, oleic acid	inhibit P-gp high affinity between lipids or NLC and cell membrane	*in-vitro*	[135]
	stearic acid, Pluronic F68, HPESO	not inhibit or bypass P-gp not alter cell membrane permeability drug released from outside of cell and then simple passive diffusion phagocytosis GG918 (P-gp inhibitor)	*in-vitro*	[136–138]
Gold NP	—	change or modify cell membrane properties dysregulate mitochondrial function	*in-vitro*	[152]
	—	internalization NPs even enter the nucleus	*in-vitro*	[153]
	—	drug-NP complex formation phagocytosis simple diffusion	*in-vitro*	[154, 155]
Silica NP	—	endocytosis bypass P-gp	*in-vivo*	[157]
	—	PEI (proton sponge effect) P-gp siRNA	*in-vitro*	[158]
	—	inhibit P-gp micropinocytosis	*in-vivo*	[159]
	—	perinuclear localization BCL-2 siRNA	*in-vitro*	[160]